Controlling Microbial Dynamics through Selective Solute Transport Across Functional Nanocultures

Shanna-Leigh Davidson[1], Tagbo H.R. Niepa[1,2,3,4,5,6]*

[1]Department of Chemical and Petroleum Engineering, [2]Department of Bioengineering; [3]Department of Civil and Environmental Engineering; [4]Department of Mechanical Engineering and Materials Science; [5]Center for Medicine and the Microbiome, [6]McGowan Institute for Regenerative Medicine, University of Pittsburgh, Pittsburgh, United States

*Corresponding author: tniepa@pitt.edu

Keywords: microbial dynamics, microfluidics, nanocultures, poly(dimethylsiloxane), chemical functionalization, Flory-Huggins.

ABSTRACT: The need for assessment tools for microbial dynamics has necessitated the miniaturization of cell-culturing techniques, and the design of microsystems that facilitate the interrogation of microorganisms in-well-defined environments. The nanocultures, as described in this work, are such an assessment tool: nanoliter-sized microcapsules generated using a flow-focusing microfluidic device to sequester and cultivate microbes in a high-throughput manner. By manipulating the chemistry of their polymeric shell, the nanocultures can be designed to achieve functionalities, such as selective permeability facilitating the transport of metabolites and other small molecules essential to control cell growth and characterize community dynamics. In this work, the transport properties of a Poly(dimethylsiloxane)-based membrane functionalized with N, N-Dimethylallylamine (DMAA) have been examined by investigating the diffusion of selected molecules relevant to controlling cell dynamics, including antimicrobials, fluorescent staining probes and sugars. Furthermore, the Flory-Huggins Interaction Parameter was evaluated as a predictive tool to elucidate the partitioning and transport of selected molecules into the nanocultures. Diffusion of molecules was confirmed experimentally by generating nanocultures containing *Escherichia coli* cells, whereby cell growth was used as a proxy for determination of successful molecule diffusion. In our study, we determined that the Flory-Huggins interaction parameters can accurately predict the diffusion of a subset of molecules across PDMS membrane; notably, those with an interaction parameter below a designated critical threshold. However, the prediction becomes less accurate as interaction parameters increased. Overall, these findings will

pave the way in our understanding of effectively using the nanocultures to study complex synergistic and antagonistic microbial behaviors in both natural and synthetic communities, with the goal of better simulating natural microenvironments and increasing discoverability of unknown molecules that are relevant to complex microbial communities.

1 INTRODUCTION

In the last two decades, technologies for the miniaturized cultivation of microorganisms in the form of 3D artificial microenvironments have evolved as assessment tools for microbial dynamics has necessitated.[1] These miniaturized tools provide access to the local physical and chemical microenvironment of microbial cells, which plays a pertinent role in community behavior, population evolution and persistence in the environment. Particularly, mass transport of chemical signals and subsequent chemical gradients effect intercellular interactions, leading to deterministic phenotypic and spatial heterogeneity within a community.[2] Within microcolonies, chemical signals alter community behavior by inducing responses such as quorum sensing, pathogenic switching, population persistence, antibiotic resistance, and nutrient cycling.[3] Furthermore, chemical signaling induces biofilm formation, whether beneficial (soil, wastewater, and oil-spill bioremediation), or pathogenic and destructive (dental plaque, infected medical devices, chronic wounds, cystic fibrosis patients, as well as fouling of pipes and ships' hulls).[4] These complex microbial relationships demonstrate the need for culturing platforms that allow for finely controlled interactions with chemical stimuli to study community dynamics in a high-throughput manner.

Droplet microfluidics is one such technology that addresses some of these needs, boasting high-throughput generation and screening, reduced reagent and sample use, and isolation and compartmentalization of cells.[5] Most importantly, microfluidics provides optical access under a microscope with the use of translucent materials such as poly(dimethylsiloxane) (PDMS), allowing for the manipulation of microbial consortia in real-time.[6] We have, therefore, developed microfluidic water-oil-water (w/o/w) double-emulsion, nanoliter-sized microcapsules, termed nanocultures, for the sequestration and study of synthetic microbial consortia.[7, 8]

The nanocultures are formed with a robust, semi-permeable polymeric (PDMS) membrane, the nature of which is to facilitate the transport of nutrients, waste, and other small, biologically relevant molecules into and out of the nanocultures. We have further enhanced the transport

capabilities of the polymeric membrane with the addition of N, N-dimethylallylamine (DMAA), whereby chemical functionalization of the membrane allows for specialized transport properties according to the required application of the nanocultures.[9] In this case, the addition of DMAA into the membrane caused the polymer to incur a larger free volume within the crosslinked network. Hence, transport properties of the membrane were modified such that small molecules, such as tetracycline, were permeable through the membrane only after functionalization with chemical modifier DMAA.[9] Although we have observed these changes in the transport properties of the polymer membrane experimentally, there is a lack of theoretical understanding of the diffusion mechanisms of small molecules across the polymeric shell of the functional nanocultures. Therefore, development of the nanocultures as a microbial assessment tool requires that we gain critical understanding of how mass transport of low molecular weight solutes partition into and permeate through the shell membrane.

For polymer-solvent binary systems, the Flory-Huggins lattice-based mixing theory is commonly used to describe thermodynamic mixing interactions.[10, 11] Recently, however, it has been expanded to relevant pharmaceutical systems, whereby the Flory-Huggins interaction parameter is used to describe miscibility and solubility of active pharmaceutical ingredients, with poor hydrophilic properties, in polymeric matrices to develop stable amorphous drug formulations.[12-15] Various methods are used to explore miscibility of drug-polymer binary systems at ambient temperatures; however, most include tedious experimental techniques, such as solid-state NMR spectroscopy, the melting depression method, and glass transition temperature measurements by differential scanning calorimetry.[15] Other qualitative methods utilize complex computational data mining to elucidate drug-polymer miscibility, which presents its own challenges when data for specific systems are unknown.[16] A more direct, quantitative method to predict miscibility of drug-polymer systems is to approximate Flory-Huggins interaction parameters through the calculation of Hansen Solubility Parameters (HSP).[17, 18] Calculating Hansen Solubility Parameters using the Group Contributions method requires only knowledge of the chemical structure of the solute, thereby increasing the usability of this method for molecules whereby thermodynamic data is unavailable.[19] Although lattice-based solution models are now well described to determine solute-polymer miscibility in binary systems, there has been slow progress in their application to multi-component systems,[20] such as ours that include the polymer

and solute solvated in water. Therefore, we aim to apply the Flory-Huggins mixing theory to our system, to investigate diffusion of small molecules across the nanoculture polymeric membrane.

The objective of this study is to investigate the Flory-Huggins interaction parameter as a predictive tool to measure the miscibility of biologically relevant molecules with the nanoculture polymeric membrane and to experimentally corroborate the same. Flory-Huggins interaction parameters were calculated for a set of biologically relevant molecules, including antibiotics, fluorescent probes, and sugar molecules, whereby a threshold value was determined to predict miscibility and permeability of the compounds. Diffusion of the same molecules was evaluated experimentally by generating nanocultures containing *Escherichia coli* cells, whereby fluorescence intensity of the cells was measured as a proxy for cell growth.

This work lays the foundation in understanding chemical transport across functionalized PDMS membranes. We hypothesize that this second generation of functional nanocultures will provide improved access to synthetic and natural microbial consortia in precisely controlled microenvironments to study complex synergistic and antagonistic microbial behaviors. With the development of nanocultures, we aim to better simulate natural microenvironments for the increased discoverability of metabolic potential within a community, such that pertains to drug discovery and high-throughput screening of biological and chemical assays, as well as the development of therapeutic nanocultures which may secrete beneficial bioactive components.

2 RESULTS AND DISCUSSION

2.1 Determining Flory-Huggins Interaction Parameters for Solute-Polymer Permeability

Although the nanocultures present a unique platform for multi-component drug-polymer miscibility, the application of the Flory-Huggins mixing theory to our system is apt, as diffusion of the solute hinges on the miscibility of the solute with the polymer. For this specific system (the nanocultures), molecular-level mixing of the solute with the polymer can be achieved with dissolution of each component in a mutual solvent, such that mixing proves thermodynamically favorable.[20] Therefore, considering the solute dissolved in water as a solvent, Flory-Huggins interaction parameters may be used to develop a predictive model for diffusion of small molecules

through the polymer lattice. A predictive tool such as this based simply on molecular structure of the compounds would be broadly beneficial to our system: experimental times would be significantly decreased if controls to test diffusion were negated based on the predictive power of the Flory-Huggins interaction parameter. This would allow for targeted design of nanocultures for specific applications, providing access to some molecules, but not others, in the independent study of environmental stimuli on microbial community dynamics. Therefore, we have calculated the Flory-Huggins interaction parameters for several selected molecules to determine the predictive power of the interaction parameter for diffusion of solutes across the nanoculture membrane. The molecules selected for this study are biologically relevant to controlling microbial dynamics and cell growth, as well as differential contrast staining for the assessment of microbial growth dynamics and include antibiotics, fluorescent probes, and sugar molecules.

The Flory-Huggins interaction parameter, χ, depends on the HSP, δ, of both the solute (component 1) and polymer (component 2) as in the following relationship:

$$\chi = \frac{V_1(\delta_1 - \delta_2)^2}{RT}, \qquad (1)$$

where V_1 is the molar volume of component 1, R is the real gas constant, and T is the absolute temperature (Supporting Information).[11] The interaction parameter, χ, represents the enthalpic contribution to the Gibbs free energy of mixing, which, furthermore, requires that total Gibbs free energy of mixing be less than 0 for miscibility to occur.[14] Hence, χ must be 0, or significantly small such that the enthalpic contribution does not offset entropic gains that facilitate mixing. According to the Flory-Huggins mixing model for polymer-solute systems, the critical interaction parameter (χ_{crit}) will be system-specific, as defined by the size of the lattice.[20] However, for systems using PDMS, a critical interaction parameter of $\chi \leq 0.5$ has been suggested as an indicator of miscibility.[17, 21] To achieve such small values of χ, one can infer from Equation 1 that solutes exhibiting similar solubility parameters, δ, to the polymer, are anticipated to overcome intermolecular cohesive forces ("like dissolves like") and permeate through the polymer membrane.

To determine χ of each selected molecule with PDMS, total solubility parameters must be calculated for the selected molecules. Determining HSPs for biologically relevant molecules may be challenging; whereas solubility parameters for low molecular weight liquids can be

conveniently found experimentally by obtaining the heat of vaporization, such direct methods do not work for high molecular weight polymers and crystal powders due to their low volatility.[17] Therefore, a common indirect method for estimating δ for such materials is based on Fedor's group contribution "molar-attraction constants" method, whereby only the chemical structure of the compound is needed to sum the molar attractions of each functional group.[22] Since the development of the group contributions method, it has evolved through many iterations to become an accurate tool in estimating several thermodynamic properties of compounds.[17, 18, 22-26] A crucial enhancement to the understanding of total solubility parameters was the development of Hansen's partial solubility parameters which better describe the different intermolecular forces governing a molecule. It is now widely understood that three kinds of intermolecular forces exist: dispersive, polar, and hydrogen-bonding forces, all of which play an integral role in the thermodynamic properties of materials. Thus, the total solubility parameter, δ_t, is expanded upon as such:

$$\delta_t = \sqrt{\delta_d^2 + \delta_p^2 + \delta_h^2} \qquad (2)$$

where δ_d represents dispersive forces, δ_p represents polar forces and δ_h describes hydrogen bonding forces (Equation 2). Accounting for these three forces results in a significantly more accurate estimate for the total solubility parameter and subsequently the predictive power of the Flory-Huggins interaction parameter has larger capacity.[18]

Partial solubility parameters, as well as molar volumes of the compounds of interest were kindly provided by Prof. Steven Abbott (HSPiP), whereby the software HSPiP delivers solubility parameters based on the aforementioned "group contributions" method. The total solubility parameter for PDMS was taken to be 7.3 $cal^{1/2}$ $cm^{-3/2}$, corresponding to 14.93 $J^{1/2}$ $cm^{-3/2}$, as reported in literature,[21] with the justification that the repeating unit used for the calculation of total solubility parameters remains unchanged in the PDMS membrane, and the assumption that the addition of 10% DMAA is negligible to the total cohesive energy of the polymer. The solubility parameters were then used to calculate Flory-Huggins interaction parameters, shown in **Table 1**. Certain limitations to the group contributions estimation method result in some compounds that cannot be accurately estimated; Stefanis *et al.*[18] describe that the group contributions method may only be accurately applied to organic compounds with three or more carbon atoms, and molecules that dissociate to form electrostatic interactions are also thought to have inaccurate HSPs.[20] Therefore,

small polar molecules (hydrogen peroxide), those that dissociate into salts (crystal violet and propidium iodide), and the proprietary compounds (molecular probe Syto 9, Thermofisher, Inc.) may not have accurately estimated HSPs. These limitations present challenges to the development of the predictive model; however, diffusion of the molecules was still investigated experimentally.

Table 1. Calculated Flory-Huggins interaction parameters for molecules of biological interest and DMAA-functionalized PDMS. The χ-parameter for water-PDMS (χ = 7.85) provides a critical threshold value and calculated χ-values smaller than this threshold are predicted to be miscible with the PDMS.

Molecule	**MW (g/mol)**	**V_s (cm^3/mol)**	**δ_d $(J/cm^3)^{1/2}$**	**δ_p $(J/cm^3)^{1/2}$**	**δ_h $(J/cm^3)^{1/2}$**	**δ_t $(J/cm^3)^{1/2}$**	**χ**
PDMS	-	-	-	-	-	**14.93**	-
Water	18.02	18.00	15.50	16.00	42.30	47.81	7.85
Antimicrobials							
Ampicillin	349.41	258.60	18.97	9.39	10.69	23.71	8.04
Chloramphenicol	323.13	213.30	19.96	14.27	11.60	27.14	12.82
Hydrogen Peroxide	34.0147	-	-	-	-	-	-
Lactic Acid	90.08	73.80	17.45	11.12	22.39	30.49	7.20
Ofloxacin	361.37	272.50	19.44	8.41	9.56	23.24	7.58
Tetracycline	444.44	317.50	20.06	16.16	15.82	30.23	29.97
Tobramycin	467.52	397.20	17.65	9.23	9.18	21.93	7.85
Fluorescent Dyes							
Acridine Orange	265.35	237.10	20.17	3.16	6.36	21.38	3.98
Crystal Violet	407.98	-	-	-	-	-	-
Nile Blue	319.40	262.20	19.19	6.86	6.87	21.51	4.57
Nile Red	318.37	248.30	20.37	5.55	5.21	21.75	4.65
Propidium Iodide	668.40	-	-	-	-	-	-
Syto-9	-	-	-	-	-	-	-
Carbohydrates							
Arabinose	150.13	121.80	17.87	13.87	25.60	34.16	18.17
Glucose	180.16	169.90	16.83	11.13	22.75	30.41	16.42
Sucrose	342.30	303.30	16.81	10.02	17.98	26.58	16.59

The units for δ are expressed in terms of energy, whereby the conversion factor is 1 $cal^{1/2}cm^{-3/2}$ = 0.488 88 $J^{1/2}cm^{-3/2}$.

Although miscibility of drug-polymer binary systems has been suggested at low critical thresholds, an investigation by Thakral *et al.*[14] established that some molecules with χ values as high as 4.19 still proved miscible with PEG 6000. Hence, solute-polymer miscibility may occur at χ values significantly higher than the theoretical threshold of 0.5, as is further demonstrated in

previous works highlighting water diffusion across PDMS membranes.[7, 27, 28] Water, as a solvent, presents an interesting case: despite its peculiar cohesive and adhesive properties due to low molar volume and strong hydrogen bonding (δ_h)[17], the HSP values for water are readily available. Hence, the diffusivity and associated χ-value for water could be used as an arbitrary measure of mass transport in our water-PDMS-water system. Thus, we have calculated the Flory-Huggins interaction parameter for the water-PDMS pair and use this value as the starting threshold to predict diffusivity for other selected molecules, since water readily diffuses across the membrane. Therefore, the χ-value, calculated to be 7.85, was arbitrarily designated as the critical threshold for this system. We hypothesize that all molecules with χ values smaller than 7.85 are predicted to be permeable. Based on this threshold, three out of the seven antibiotic molecules selected are predicted to be permeable, including lactic acid, ofloxacin and tobramycin. Furthermore, all three of the fluorescent probes with successfully calculated χ parameters are predicted to be permeable, including acridine orange, Nile blue, and Nile red. In contrast, all three carbohydrate molecules, arabinose, glucose, and sucrose, have large χ parameters and consequently, are predicted not to be permeable in the nanoculture system (**Table 1**).

These values provide invaluable information for determining the predictive power of the Flory-Huggins interaction parameter as a finite measure of the "likelihood" of solute miscibility and their subsequent diffusion across our PDMS-based nanoculture system.

2.2 Generation of polymeric double emulsion nanocultures

Monodisperse, double emulsion droplets are formed using a glass capillary microfluidic platform that generates flow-focusing, co-axial flow of the three liquid phases. Aqueous bacterial samples are encapsulated within a polymeric membrane, resulting in water-oil-water (w/o/w) microcapsules. The inner-most phase contains the sample of microorganisms suspended in a nutrient-rich broth (**Figure 1A**). The polymer developed for the containment of cells in this case is comprised of crosslinker methylhydrosiloxane-dimethylsiloxane copolymer, trimethylsiloxy-terminated polydimethylsiloxanes (HMS-053, Gelest Inc.) and vinyl-terminated polydimethylsiloxanes base (DMS-V21, Gelest Inc.) in a ratio of 1:0.6, as calculated by concentration of their functional groups, and is further functionalized with 10% DMAA.[9] Crosslinking of the polymeric membrane results in a mechanically robust, semi-permeable capsule for housing the microbes in question, and further allows the direct investigation of functional

molecules on microbial dynamics. In this study, the nanocultures range from 0.84 – 5.2 nL, with an average volume of 2.01 ± 1.27 nL, depending on controllable volumetric flow rates within the microfluidic device (**Figure 1B,C**). The nanocultures result in isolated "bioreactors" which provide ideal conditions for testing independent diffusion properties of the relevant small molecules across the polymeric membrane.

For all experiments, nanocultures were generated with *E. coli* as our model organism. Fluorescence intensity was quantified as a proxy for cell growth and subsequently, used as an identifier for molecule permeability through the nanoculture membrane.

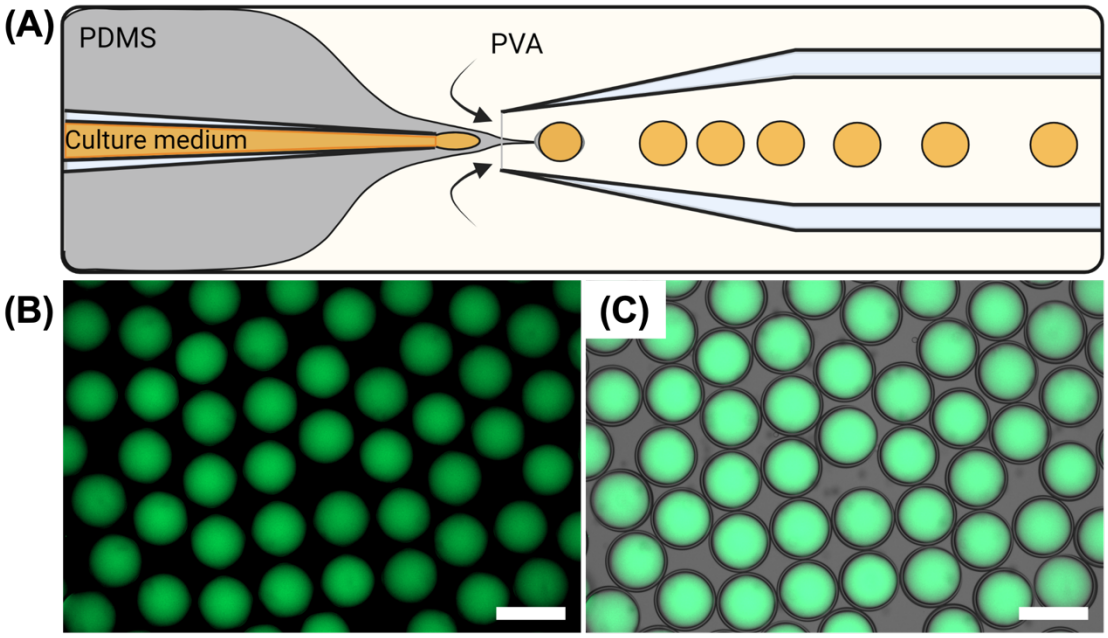

Figure 1. Generation of functional nanocultures. (**A**) Illustration depicting the microfluidic platform that allows flow-focusing at the interface of the three phases to generate double emulsion w/o/w droplets. Illustration created with BioRender.com (**B**) Fluorescent and (**C**) merged images taken at 5× (Scale bar: 200 μm) showing confluent growth of GFP- and RFP-tagged *E. coli* within nanocultures. The nanocultures are monodisperse and have equal shell thickness; however, each nanoculture acts as an isolated bioreactor.

2.3 Experimental Diffusion of Biologically Relevant Molecules

2.3.1 Antimicrobials

The ability to control diffusion of small molecules across the nanoculture membrane is pertinent to controlling both microbial dynamics within the nanoculture, as well as microbial dynamics in the external environment. Niepa et al.[7] showed previously that diffusion of small molecules across the nanoculture membrane affected cell growth rate and confluence within the nanocultures. Incubation of the nanocultures in the supernatant of a mature, overnight flask culture resulted in increased cell confluence within the nanoculture, suggesting synergistic growth

interactions. Conversely, antagonistic behaviors were seen between bacteria *Pseudomonas aeruginosa* and yeast *Candida albicans*, demonstrating the ability of the nanocultures to decouple between physicochemical interactions. The next step in the targeted design of the nanocultures is to determine the permeability of biologically relevant molecules, such that we may use the nanocultures to increase the discoverability of secreted metabolic products, particularly those that might be therapeutically advantageous. Although compounds that do exhibit permeability may be experimentally more enticing, compounds that are not permeable across the nanoculture membrane are just as important, so that the cell growth in the external environment may also be precisely controlled. For example, conditions calling for sterility in the external environment may be achieved with the use of non-permeable antibiotics. Likewise, specific co-culturing conditions may be achieved with the inclusion of spatial segregation between cells.

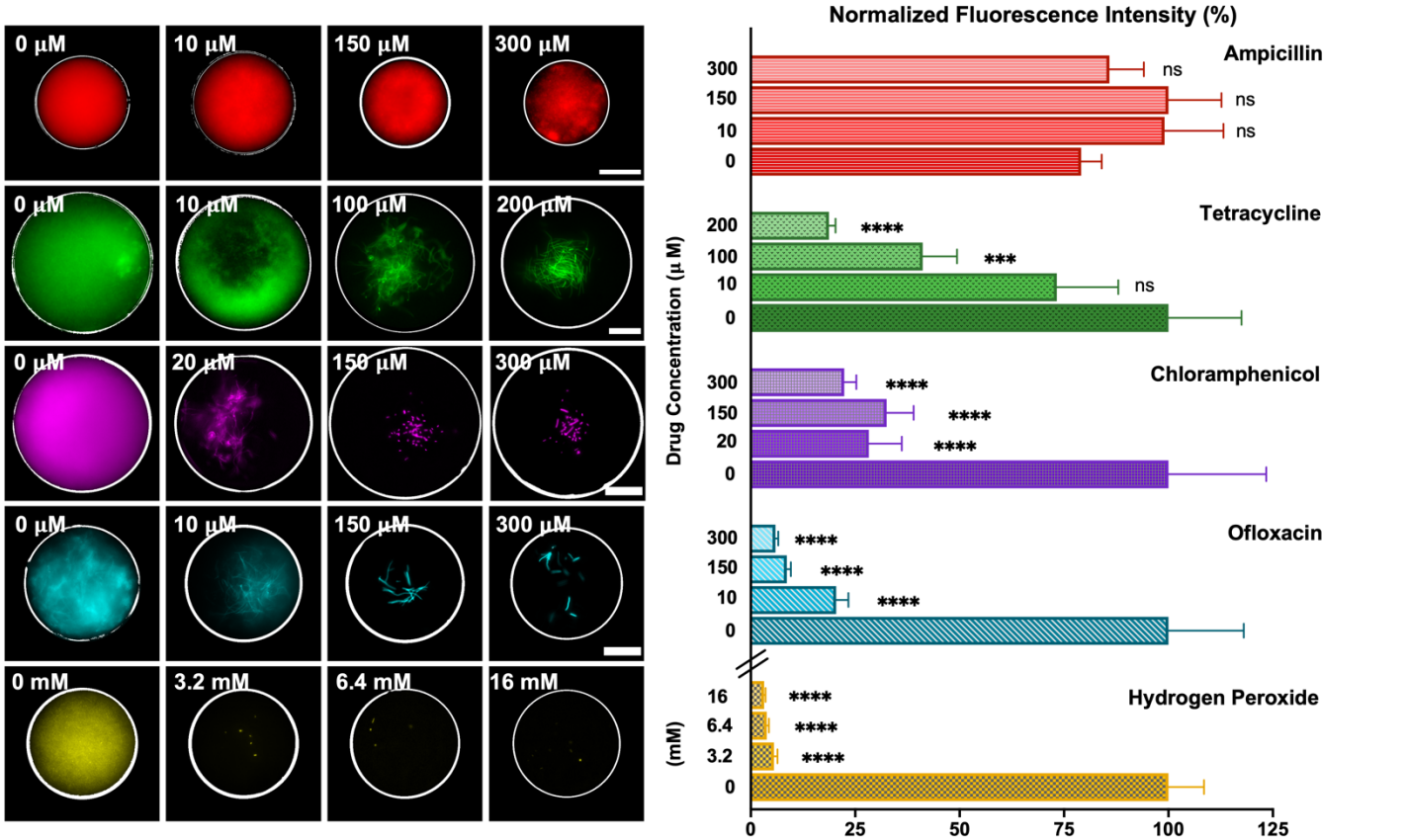

Figure 2. Left panel. Cell growth of GFP- and RFP-tagged *E. coli* cells inhibited by antimicrobial diffusion into the nanocultures. Fluorescent images taken at 50× (Scale bar: 50 µm) show nanocultures treated with antibiotics at concentrations of 0 - 16 mM, including ampicillin (red), tetracycline (green), chloramphenicol (purple), ofloxacin (light blue), and hydrogen peroxide (yellow). Images are pseudocolored to distinguish between drug treatments. Right panel. Bar plot shows mean fluorescence intensity, which was measured as a proxy for relative cell growth of nanocultures treated with antimicrobials compared to negative controls (nanocultures not exposed to antimicrobials). Fluorescence intensity is expressed as a percentage, normalized to the sample with highest fluorescence intensity per antimicrobial grouping. Differences were considered significant when $p < 0.05$. Two-way ANOVA, Tukey post-hoc, n=15 for all groups.

To determine diffusion of antimicrobials through the PDMS membrane, cell growth, or inhibition thereof, was measured by mean fluorescence intensity as a proxy. The nanocultures were generated with fluorescently tagged *E. coli* cells and incubated at 37°C for 24 hours in collection media containing the selected antimicrobial compounds. All antimicrobials were tested in concentrations ranging from 0 – 16 mM. Prior to testing diffusivity of antimicrobials through the nanoculture membrane, the antimicrobials were tested in 48-hour growth curves with the selected *E. coli* strain to ensure susceptibility to the antibiotic compounds and to determine minimum inhibitory concentrations for 50% of cell growth (MIC_{50}) (Supporting Information, **Figure S1**), dictating antimicrobial concentrations to be used in the diffusivity studies. Cell growth inhibition by the antimicrobial of interest was determined by measuring mean fluorescence intensity for the total interior area of the nanoculture. Mean fluorescence intensity was normalized to the largest value of intensity, per antibiotic grouping. As can be seen in **Figure 2**, high cell confluence within the nanocultures is shown by high fluorescence intensity. Inhibition of cell growth is subsequently depicted by decreased fluorescence intensity, with single cells becoming more apparent as compared to the nanocultures with high cell confluence.

According to our chosen critical threshold, $\chi = 7.85$, the Flory Huggins interaction parameters predict that only ofloxacin and tobramycin would be permeable through the nanoculture membrane (**Table 1**). As is observed in **Figure 2**, this is indeed the case for ofloxacin ($MIC_{50} < 2$ μM), whereby fluorescence intensity decreased by more than 75% ($p < 0.0001$) at 10 μM antibiotic. In contrast, although the χ parameter for tobramycin is 7.85, identical to that of water, Manimaran et al.[9] has previously shown, using a similar system containing bacteria encased in polymeric microcapsules, that tobramycin is not permeable through the DMAA-functionalized shell membrane. For this reason, tobramycin was omitted from the experimental diffusivity studies here. Furthermore, calculated χ parameters predict that ampicillin, chloramphenicol, and tetracycline will each be impermeable through the membrane. As is observed, this is the case for ampicillin (MIC_{50} ~72 μM), whereby no significant decrease in cell growth is determined. This is a particularly interesting result, because in first generation nanocultures produced with commercial polymer Sylgard 184™, Niepa et al.[7] showed that ampicillin readily diffuses through the membrane. Hence, the polymer membrane functionalized with DMAA has been modified such that the chemical interaction with ampicillin no longer permits permeability through the

membrane. This further demonstrates that a fundamental understanding of small molecule diffusion is needed to make a robust and accurate predictive tool.

In contrast, tetracycline, and chloramphenicol both exhibit permeability through the membrane. This is most obvious in the case of chloramphenicol (MIC_{50} ~10 μM), whereby fluorescence intensity is significantly decreased ($p < 0.0001$) at the lowest antibiotic concentration, 20 μM. Furthermore, nanocultures incubated with chloramphenicol and ofloxacin ($MIC_{50} < 2$ μM) at a concentration of 20 μM and 10 μM, respectively, exhibit cell stress, whereby bacterial cells do not divide properly and present with long, string-like growth,[29] further confirming permeability of the two antibiotics. Although tetracycline did prove permeable, 100 μM of the antibiotic was required to achieve similar cell stress and growth inhibition. However, supplementary growth curves with tetracycline show that the MIC_{50} may be as low as 2 μM (Supporting Information, **Figure S1**). Therefore, for such high concentrations of tetracycline to be required to achieve cell growth inhibition within the nanocultures, we hypothesize that the polymer membrane affords some level of protection to the microbial cells in some cases, but not all. The mechanism by which this occurs is interesting but provides a challenge in understanding why diffusion of some molecules is inhibited, whilst others diffuse readily. The χ parameter for hydrogen peroxide was unable to be calculated due to strong polar bonding; however, diffusion occurred readily through the membrane and inhibited cell growth at all concentrations (**Figure 2**).

Cataloguing diffusion of molecules in this way offers an opportunity to carefully select for antibiotics, such as ampicillin and tobramycin, that can be used to control sterility of the external environment of the nanocultures without affecting microbial dynamics within the nanocultures. The design of this system allows each nanoculture to be used as an ideal, isolated bioreactor that may be probed with a variety of external stimulants and studied with simple optical techniques using light and fluorescence microscopy. Furthermore, controlling selective permeability of the membrane allows for the creation of synthetic microbial consortia with a defined metabolic profile, relevant for designing therapeutic nanocultures with a specific chemical profile.

2.3.2 Fluorescent staining dyes

Fluorescent stains are integrative to the study of microbial cells and range in application from determination of cell viability and enzymatic metabolic reactions to omics methods that rely on fluorescence for quantification, such as quantitative PCR (qPCR), flow cytometry and

fluorescence in situ hybridization (FISH).[30] The fluorescent dyes chosen for this study are useful for applications of the same, and therefore, diffusivity of these molecules across the nanoculture membrane indicates the development of the nanocultures as an optimal, high-throughput assessment tool. In the LIVE/DEAD BacLight Bacterial Viability Kit (ThermoFisher), propidium iodide and Syto 9 are used as complementary agents to determine cell viability in a sample, whereby Syto 9 is cell-membrane permeable and stains green total nucleic acids whilst propidium iodide contrast-stains red only cells with damaged membranes. The cationic dyes such as Nile blue, Crystal Violet and Acridine Orange localize in negatively charged cellular organelles, and therefore, are prominent in the analysis of cellular physiology and cell cycle status.[31] Acridine Orange has the added benefit of being metachromatic, such that binding with double-stranded DNA results in emission of green fluorescence (520 nm), whereas binding with single-stranded DNA or RNA results in emission of red fluorescence (650 nm). Furthermore, due to its cationic properties, Acridine Orange may also localize in acidic compartments, whereby low pH conditions result in orange fluorescence emission.[32] These dyes may also be used for live cells; therefore, the nanocultures present an opportunity to evaluate changes in fluorescence emissions in real-time over relevant temporal scales.

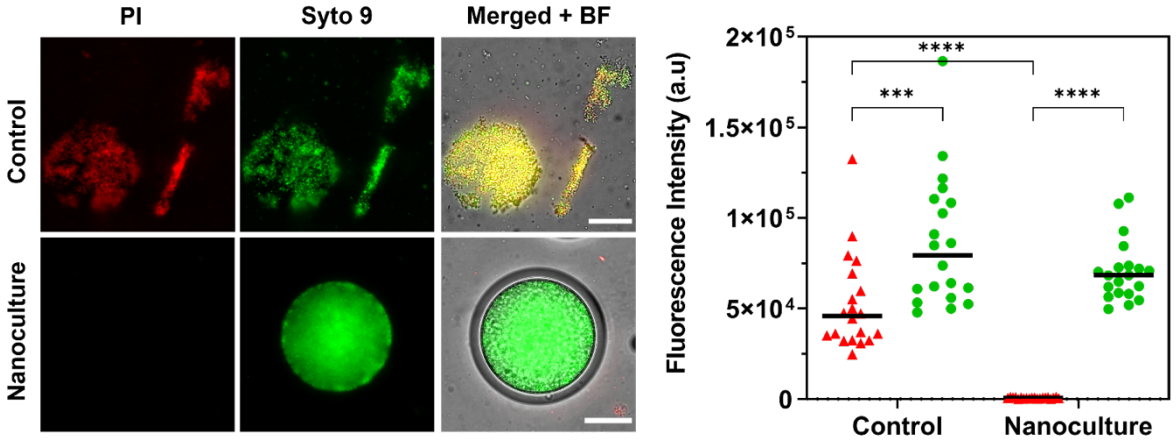

Figure 3. Nanocultures treated with LIVE/DEAD BacLight Bacterial Viability Kit (Propidium Iodide and Syto 9). Fluorescent and brightfield (BF) images taken at 50× (Scale bar: 50 μm) show that propidium iodide (1.5 μL/mL) is unable to permeate the nanoculture, membrane, whereas Syto 9 (1.5 μL/mL) readily diffuses to stain the encapsulated *E. coli* cells. Scatter plot shows mean fluorescence intensity measured for a non-encapsulated control and the nanocultures. Red triangles indicate Propidium Iodide fluorescence. Green circles indicate Syto 9 fluorescence. Differences were considered significant when $p < 0.05$. Two-way ANOVA, Tukey post-hoc.

Permeability of chosen fluorescent dyes (**Table 1**) was determined qualitatively by evaluating fluorescence of the nanocultures after incubation with the fluorescent probe through imaging. Nanocultures were generated with wild type *E. coli* Nissle 1917 cells (non-fluorescent) and were

cultured for 24 hours at 37°C to achieve cell confluence. Fluorescent dyes were then added to the external collection solution and left to incubate at room temperature for 30 minutes. The samples were imaged with brightfield and fluorescent channels and fluorescence intensity was measured in ImageJ.

Table 1 shows calculated values for the Flory-Huggins interaction parameters (χ) for those molecules that could be calculated. χ-values for molecules that dissociate into ionic salts, such as crystal violet and propidium iodide, were unable to be calculated.[18] Furthermore, the interaction parameter for Syto 9 could not be calculated due to the proprietary nature of the compound. Despite this, experiments showed that Syto 9 (**Figure 3**) and crystal violet (**Figure 4**) are both permeable through the membrane of the nanocultures, whereas propidium iodide exhibited impermeability. To ensure that the viability stains were working as intended, a positive control sample of bacteria was stained in parallel (Supporting information, **Figure S2**). **Figure 3** shows that control cells not encapsulated could be stained simultaneously with propidium iodide and Syto 9, whereas cells grown within nanocultures were unable to be stained with propidium iodide ($p < 0.0001$). This presents some challenges in viability studies, due to the complementary nature of the compounds; however, it may be possible to circumvent this issue by preferentially using fluorescent dyes that indicate positive metabolic activity instead, such as acridine orange and resofurin.

The three fluorescent probes that could be calculated for interaction parameters, acridine orange (3.98), Nile blue (4.57) and Nile red (4.65), all exhibited the lowest interaction parameters of all molecules and suggest that diffusion should occur readily. This was indeed the case when tested experimentally. In control experiments, the three fluorescent probes can successfully stain wild-type *E. coli* Nissle cells that were not encapsulated (Supporting information, **Figure S2, S3**). Surprisingly, despite acridine orange having the lowest calculated χ parameter, its diffusion into the nanocultures did not occur within the initial 30-minute incubation period, as the other fluorescent probes did. We, therefore, hypothesized that the functionalized polymer membrane was inducing an unknown interaction with the molecule that inhibited diffusion to a small extent, much like in the case of tetracycline. Subsequently, we measured fluorescence intensity within the nanoculture over time to determine the minimum amount of time that was needed to achieve diffusion. Measured at 520 nm for green fluorescence (dsDNA-bound) and 650 nm for red

(ssDNA- or RNA-bound),[31] diffusion of acridine orange was primarily observed after 60 minutes; however, took approximately 360 mins to reach maximum fluorescence intensity (**Figure 4**).

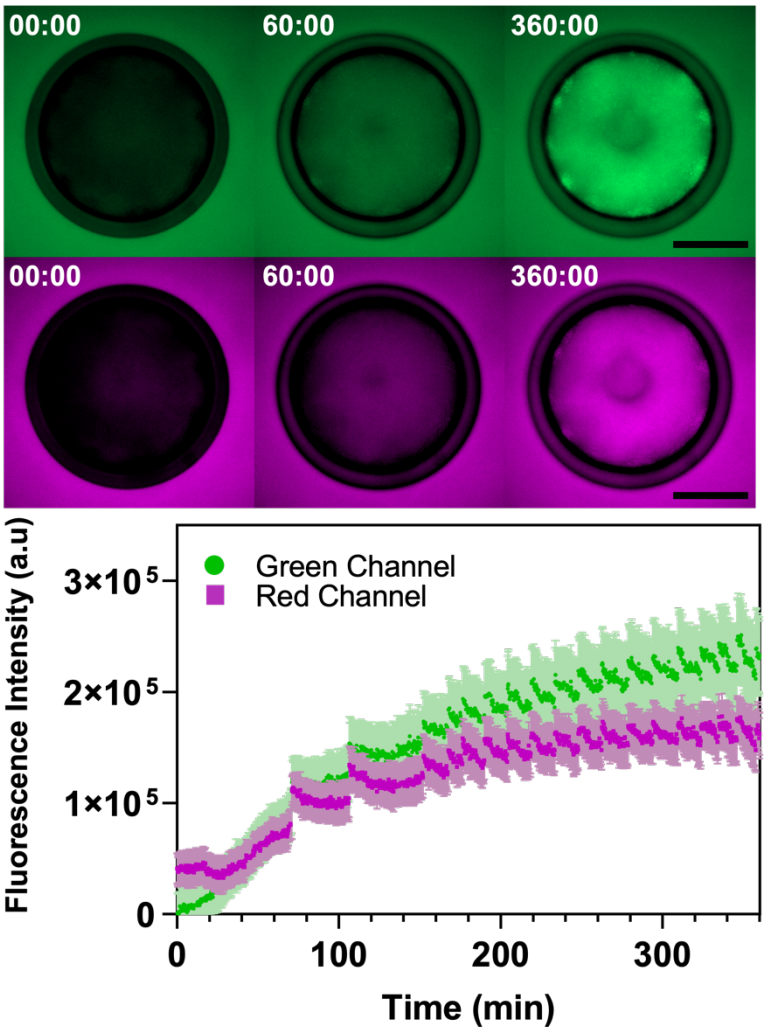

Figure 4. Time lapse of acridine orange diffusion into the nanocultures. Acridine orange (15 μM) is a metachromatic dye that emits fluorescence at different wavelengths depending on its activity. Green emission (520 nm) indicates that it is double-stranded DNA-bound, whereas red emission (650 nm) indicates that it is single-stranded DNA- or RNA- bound, providing insight into metabolic activity of the cells. Red channel pseudocolored to magenta to increase readability. Nanocultures were observed for 360 mins, and initial fluorescence can be seen after 60 mins of incubation. Fluorescent images taken at 50×. Scale bar: 50 μm.

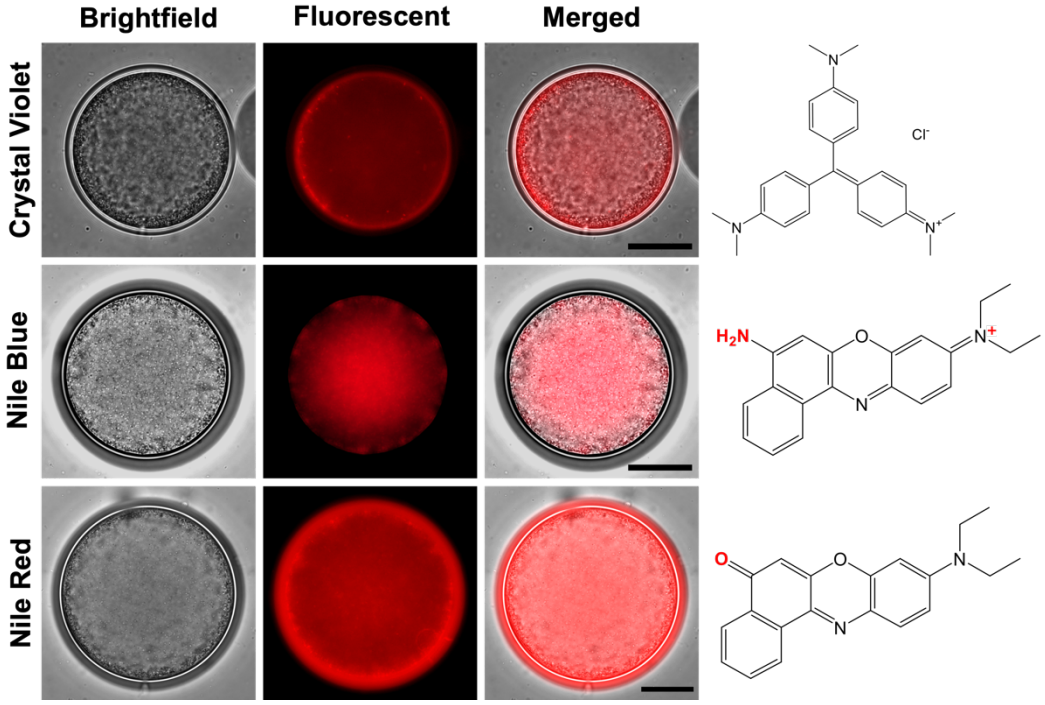

Figure 5. Nanocultures treated with fluorescent probes. Fluorescent and brightfield images taken at 50× (Scale bar: 50 μm) show that crystal violet (0.5%), Nile blue and Nile red (25 μM) readily diffuse to stain encapsulated *E. coli* cells. However, even though Nile blue and Nile red are structurally similar dyes and have almost identical χ-values, they localize in different locations; Nile blue permeates entirely into the nanoculture, whereas Nile red stains the PDMS membrane itself. Although the Flory-Huggins interaction parameter predicts permeability with the membrane, χ-values cannot predict such differences in dye staining behavior.

Diffusion of Nile blue and Nile red led to a further interesting phenomenon. Both molecules, almost equal in molecular structure bar two functional groups – an amine and N+ in Nile blue and a carboxylic group in Nile red (**Figure 5**) – showed permeability through the polymer membrane. However, the fluorescent dyes localized in different places within the nanoculture. Nile blue readily diffused to stain only the bacterial cells, as expected. In contrast, Nile red localized within the polymer membrane itself, resulting in the polymer exhibiting strong fluorescence, but not the bacterial cells initially. After a longer incubation period, Nile red did partition through the membrane and successfully stain the cells; however, the PDMS membrane remained strongly fluorescent to the point that bacterial cells were indistinguishable from the membrane fluorescence. This result seems to agree with our earlier hypothesis that diffusion of molecules through the polymer membrane is being governed by other factors independent of predicted miscibility through interaction parameters alone. When taking into consideration effects of physical forces (dispersion and polar), versus chemical forces (hydrogen bonding), there seems to be a consensus

that hydrogen bonding interactions play an extensive role in permeant solubility in PDMS membranes.[20, 33] Some of these known interactions include hydrogen bonding (-OH) of the solute with oxygen in the membrane within the Si-O-Si functional core groups, as well as hydrogen bonding between oxygen (-OH) in the solute and hydrogen within Si-H functional groups in the membrane.[34] Non-polar interactions may also dictate solute-polymer miscibility and may provide some insight into the differences in localization of Nile blue compared to Nile red, where Nile red is strongly lipophilic, whereas Nile blue may experience preferentially polar interactions. The mechanisms of these interactions are, however, challenging to describe based on chemical structure alone, as most of the compounds selected for this study include functional groups that have strongly directional interactions, including amines, carboxyl groups and hydroxyl groups,[20] with no clear indication of whether the solute will be permeable. We, therefore, postulate that diffusion through the polymer is not trivial and chemical interactions between the polymer and solute may help, or hinder, diffusion of molecules.

The determination of permeable fluorescent probes through the nanoculture membrane allows the nanocultures to be utilized in several necessary contrast assays, particularly relevant for determining spatial heterogeneity of cells within the capsules and other microbial dynamics. The permeability of some fluorescent probes sets the precedent for future developments of the nanoculture membrane, such that full staining techniques may be performed. For example, performing Gram-staining or immunostaining within nanocultures, prevalent to initial characterization of unknown cells, would allow the nanocultures to be used to identify various cell types in environmental samples, whereby conventional culturing of these cells proves difficult.

2.3.3 Sugars

Another important aspect in the functionality of permeability of the nanocultures is the diffusion of carbohydrate molecules, which would impart the ability to feed microbial communities from the external environment of the nanocultures. Alternatively, withholding carbohydrate molecules would introduce a new dimension to the study of real-time dynamics, as phenotypic switching and other metabolic functions could be studied in real-time for cells undergoing stress.

We determined that cells that had no carbon source within the nanocultures would be unable to grow to any measurable confluence. Thus, to study diffusion of sugar molecules into the nanocultures, cell growth within the nanocultures was qualitatively observed through brightfield imaging. Prior to selecting an appropriate strain for diffusion experiments, 48-hour growth curves of several strains of cells were performed in M9 media supplemented with glucose (Supporting information, **Figure S4**) to ensure that cells would successfully grow, given a source of carbohydrates. The chosen strain of *E. coli* mApple (RFP) was used to generate nanocultures containing minimal M9 media, supplemented with trace vitamins, $FeSO_4$, and $CaCl_2$, ensuring that the cells had all necessary growth factors, bar carbon, in order to grow. The test sugars (glucose and sucrose) were added to the external collection media in concentrations from 0-10% (v/v), and nanocultures were incubated for 48 hours at 37℃ in aerobic conditions. Brightfield imaging of the nanocultures was subsequently performed to observe growth of the bacterial cells, the presence of which would confirm diffusion of the sugar molecules.

In addition to glucose and sucrose, diffusion of a third sugar, arabinose, was also studied as a potential external carbon source. However, fluorescence in *E. coli* mApple (RFP) is induced by arabinose. Therefore, in this case, mean fluorescence intensity was again examined as an indicator of diffusion. Nanocultures were generated using the same *E. coli* mApple (RFP) in nutrient rich UFTYE media. Arabinose (100 μg/mL) was added to the external collection media and nanocultures were incubated for 24 hours at 37℃ in aerobic conditions. Mean fluorescence intensity of the cell growth was measured, and comparisons were made for samples including and excluding arabinose.

Calculated interaction parameters for the three carbohydrate molecules (**Table 1**), glucose (16.42), sucrose (16.59), and arabinose (18.17) are relatively high - approximately 4 times larger than χ-values for the fluorescent probes, and 2.2 times larger than the established χ threshold value, 7.85. Therefore, diffusion of these sugar molecules was perhaps improbable; however, their χ-values still fall well below that of tetracycline (29.97), which did show permeability through the membrane. Despite possible theoretical permeability according to our Flory-Huggins predictive tool, no cell growth was observed for the cases of glucose and sucrose; neither of the sugars indicate permeability through the polymer membrane (Supporting information, **Figure S5**).

Likewise, arabinose also proved impermeable through the nanoculture membrane (Supporting information, **Figure S6**). The addition of arabinose to the external collection media did not lead to an increase in mean fluorescence intensity in comparison to the negative control which had no arabinose added. In contrast, a positive control with 100 μg/mL arabinose added to the core encapsulation media led to a significant increase in fluorescence ($p < 0.0001$) in comparison to both the test sample and negative control sample. It must be noted that leaky fluorescence occurred in the negative control sample (0 μg/mL arabinose); however, this fluorescence was accounted for during data analysis.

Sugars such as these tested here would be unable to feed microbial consortia from outside of the capsules; all sugars should be included in the aqueous core phase during the encapsulation process. However, the nanocultures present an interesting tool to study metabolic changes during cell stress in the absence of relevant sugar sources and could prove useful in determining how microorganisms adapt to their environment during stress.

2.4 Effects of Membrane Shell Thickness on Diffusion

We anticipated that thickness of the nanoculture shell membrane may play a role in diffusion times, as noted experimentally with the fluorescent probes, specifically acridine orange. The Flory-Huggins interaction parameter may give an estimate of initial miscibility between a solute and polymer pair; however, the associated χ-value does not provide any information as to the kinetics of the system. Hence, we sought to determine how thickness of the shell membrane may play a role in the kinetics of diffusion, as this may play a pertinent role in the development of the nanocultures as a fast and efficient tool for several screening applications, such as drug discoverability or drug susceptibility. For this purpose, we chose to use lactic acid to explore diffusion kinetics for varying membrane shell thickness, due to the broadly therapeutic relevance of lactic acid.[35, 36]

The Flory-Huggins interaction parameter for lactic acid was calculated to be 7.20, and therefore predicted to be permeable through the membrane. Noting the advantage of optical transparency of the nanocultures, we used a colorimetric assay to monitor lactic acid diffusion times through the polymer membrane by observing the neutralization reaction between lactic acid and sodium hydroxide (NaOH). The colorimetric assay utilized pH indicator thymol blue to monitor changes in pH within the core of the nanoculture throughout the diffusion experiment. At

high pH (9.6 ~13), thymol blue is a deep blue color which changes to yellow as the pH decreases to a mid-range of 9.6~2.8. Below pH 2.8, thymol blue further reduces to red, allowing us to investigate changes in pH in real-time by analyzing the color change in thymol blue. Nanocultures were generated with 0.1 M NaOH (pH 13) containing 1 mg/mL thymol blue and were collected in 0.1 M NaCl solution. Equal concentrations of dissociated ions on either side of the nanoculture membrane ensure that the induced osmotic pressure is equal across the membrane, thus preventing water flux and changes to the concentration of NaOH in the nanoculture. In this case, 0.1 M NaOH induces an osmotic pressure of 455.9 kPa, whereas 0.1 M NaCl results in an osmotic pressure of 454.9 kPa, thereby inducing a nonzero but negligibly small water flux into the capsule. 0.2 M lactic acid (pH 1.89) was then added to the external collection solution and thymol blue color change was monitored with a brightfield time-lapse. Two conditions were studied, whereby nanocultures either had an average shell membrane of 12.18 ± 3.63 μm, or an average shell membrane of 2.75 ± 0.75 μm. Color change from blue to yellow was evaluated by measuring the RGB blue channel intensity with ImageJ for the duration of the reaction. A control sample containing only 0.1 M NaOH and 1 mg/mL thymol blue and having no reaction with lactic acid was also monitored by time-lapse, to determine the diffusivity of thymol blue. As shown in **Figure 6**, the control showed stable blue intensity throughout the time-lapse, confirming the impermeability of thymol blue through the membrane.

Diffusion of lactic acid was confirmed, and the subsequent reaction between NaOH and lactic acid results in the production of sodium lactate, water, and dissociated lactate ions, effectively neutralizing both reagents within the nanoculture and resulting in a color change from blue to yellow as the pH decreases. **Figure 6** shows descriptively how diffusion occurred for the two conditions; it was observed that nanocultures with thin shell membranes (average 2.75 μm) took only 1 minute to reach equilibrium, whereas nanocultures with thick shell membranes (average 12.18 μm) took approximately 110 minutes for the reaction to reach equilibrium and for color change to remain stable. The drastic difference in time of diffusion depicted in this experiment suggests that the shell thickness has a significant effect on diffusion kinetics of small molecules, and careful consideration should be taken in the subsequent targeted design of nanocultures, as necessitated by application.

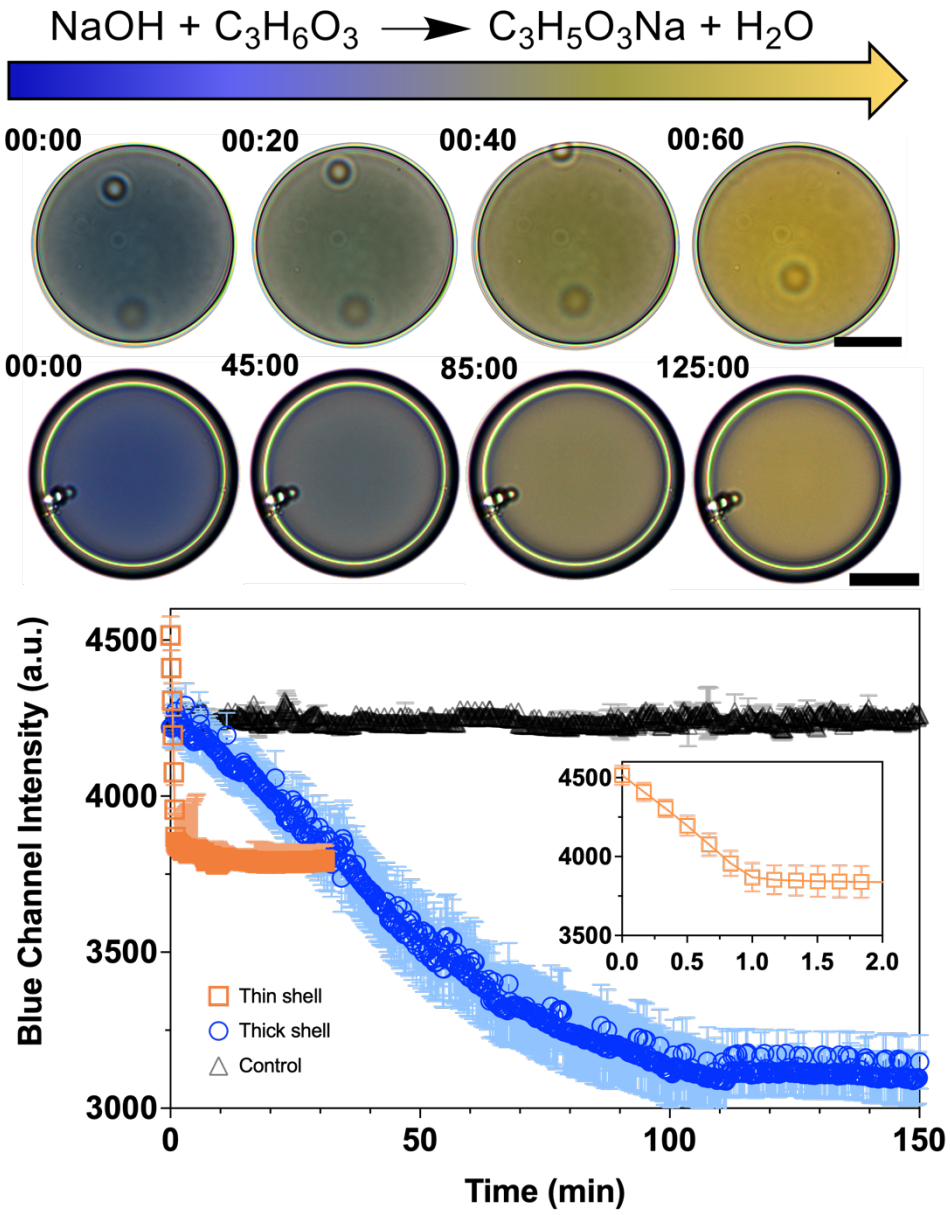

Figure 6. Diffusion kinetics of lactic acid into the nanocultures. Lactic acid was used to compare differences in diffusion based on membrane thickness. Two conditions were studied, whereby shells were thick (average 12.18 μm) or thin (average 2.75 μm). Thymol blue was used as a pH indicator to monitor reaction conditions within nanocultures. Thymol blue is non-permeable through the membrane, confirmed by the control sample with no reaction. The reaction between NaOH and lactic acid results in a pH drop, observed by the color change from blue to yellow. Diffusion for thin shells occurred rapidly, whereas diffusion with thick shells took 110 mins to reach equilibrium. Brightfield images taken at 50×. Scale bar: 50 μm.

These results lead us to believe that, not only is it necessary to be able to predict diffusion of small molecules, but to also understand differences in diffusion kinetics so that future studies utilizing assays like these develop protocols that are standardized and relevant to real clinical applications. For scale up purposes, it is important to develop methods that result in nanocultures

that are monodisperse and consistently have equal shell membrane thickness, such that results are not obscured due to lag in diffusion. For use in high-throughput screening, the thin shell membrane presents advantages in significantly decreased diffusion times, whereby assays can be performed in a matter of minutes, as opposed to hours. However, for applications in drug delivery or the like, it may be preferable to have thick shell membranes which deliberately hinder diffusion of certain molecules such that delivery time is extended, and duration of drug activity persists. Rather than achieving bolus delivery, causing the local concentration to fluctuate dramatically, stable, and extended-release delivery can be achieved. The realization of these results is that a seemingly minor change to the design of the nanocultures, such as membrane thickness, can drastically affect diffusion times, and such design parameters will be informative for the type of applications that the nanocultures will be useful for. Developing design parameters such as these is part of our ongoing work.

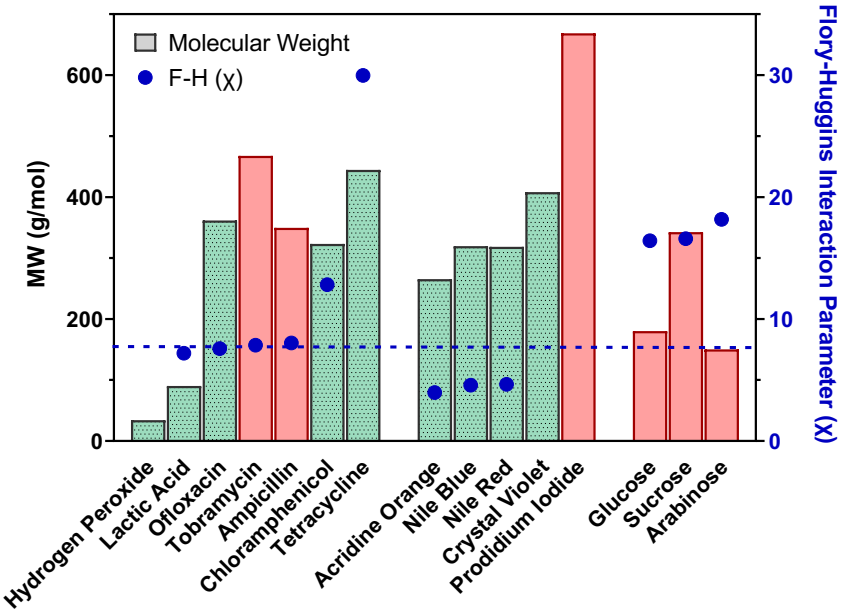

Figure 7. Summary of molecular weight vs. Flory-Huggins interaction parameter and permeability. Trends in molecular weight and Flory-Huggins interaction parameters were not sufficient to predict molecule permeability through the membrane. Dashed blue line indicates critical threshold, $\chi = 7.85$. Bars in red are impermeable through the nanoculture, whereas bars in green depict permeability. All results summarized here are from this study, with the exception of Tobramycin, which was investigated previously by Manimaran et al.[9]

2.5 Variations of Flory-Huggins Interaction Parameter

The discrepancies observed between the current Flory-Huggins predictive model and our experimental results, summarized in **Figure 7**, lead us to wonder if there is a significant divergence from the literature value for δ_{PDMS} = 7.3 $cal^{1/2}$ $cm^{-3/2}$ (14.93 $J^{1/2}$ $cm^{-3/2}$) and our functionalized, DMAA-based PDMS. Being unable to experimentally find HSPs for the polymer, it is likely that there may be some inconsistencies, further limiting the use of our Flory-Huggins predictive tool. Considering this, we hypothesized that we may potentially find an HSP value for our polymer that provides more accurate estimations for Flory-Huggins interaction parameters and subsequent miscibility with the solute. We, therefore, altered the literature-based HSP for PDMS to explore the effects of new χ-values on theoretical miscibility of solutes in PDMS.

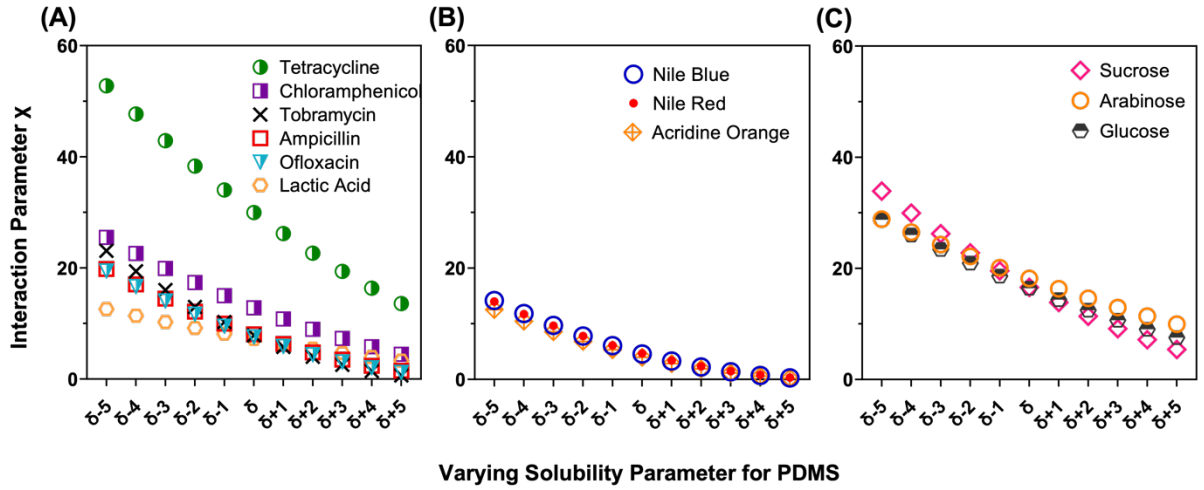

Figure 8. Variability of Flory-Huggins interaction parameters based on changing HSP values for PDMS. Due to the exact HSP value for PDMS being unknown, trends in Flory-Huggins interaction parameters were investigated for (**A**) antimicrobials, (**B**) fluorescent probes, and (**C**) sugars by changing the HSP value for PDMS in increments of 1, covering a wide range of HSP values. Trends stayed constant throughout; predictions for molecules, specifically tetracycline and tobramycin, are not altered sufficiently to improve the prediction power of Flory-Huggins.

To this purpose, we varied the δ_{PDMS}-value by adding or subtracting integers in increments of one and then compared new χ-values to our experimental results. **Figure 8** shows the change in χ-behavior over the range of ten integers for each molecule. As the HSP value for PDMS is increased, the theoretical difference between the HSP of the solute and polymer tends to zero, which subsequently results in smaller χ-values. However, in the case of the antimicrobials (**Figure 8A**), the χ-value for tetracycline remains the highest of all calculated interaction parameters. Further still, hypothetical χ-values calculated for ampicillin remain under the threshold of

chloramphenicol, despite experiments proving chloramphenicol's permeability and ampicillin's lack thereof. Moreover, χ-values for tobramycin remain below those of chloramphenicol, which would suggest permeability across the membrane; however, tobramycin remains impermeable experimentally.[9] Even at the extreme ends of the calculated spectrum of new χ-parameters, there appears to be no trend between calculated χ-parameters, and experimental diffusivity of the fluorescent probes (**Figure 8B**) and sugar molecules (**Figure 8C**). For example, all three sugar molecules would be within the theoretical range of χ-values of 10–30; however, as experiments have demonstrated, the sugar molecules tested are not permeable through the polymer membrane (Supporting information, **Figure S5, S6**).

Based on these data, we have determined that diffusion of small molecules across the polymer membrane is a nontrivial phenomenon that may not be simply explained with molecular weight nor Flory-Huggins interaction parameters. These results highlight the limitations in the development of the Flory-Huggins χ approximations to predict mass molecular diffusion in our nanoculture system. Furthermore, the challenges faced in calculating Hansen Solubility Parameters for molecules with I) strong polar bonds; II) ion-dissociating properties; and III) undisclosed proprietary chemical structures show that much work needs to be done to improve methods that may circumvent these limitations if we are to develop a successful predictive tool without the use of laborious experimental techniques.

3- CONCLUSIONS

This work aimed to investigate the use of Flory-Huggins mixing theory to develop a predictive tool to estimate solute-polymer miscibility and permeability of the solutes in a multi-component system comprised of the nanocultures and solutes in aqueous media. Double emulsion microcapsules (the nanocultures) were generated with DMAA-functionalized PDMS, providing a robust and semi-permeable shell to house *E. coli* cells. Diffusion of molecules was investigated and measured by proxy of cell fluorescence intensity, or cell growth visualized under optical brightfield conditions. The results from these experiments highlight several significant challenges in developing such a predictive tool. Firstly, limitations in the calculation of HSPs prevented subsequent calculations for χ-parameters of the pertinent molecules (25% of selected molecules).

Therefore, permeability could only be determined experimentally for these molecules. Secondly, the Flory-Huggins χ-parameter does not inform on diffusion kinetics or behaviors of small molecules through membranes, which was demonstrated experimentally to be a pertinent design parameter of the nanocultures, and which can be used to our advantage for specific applications. As the Flory-Huggins model stands currently, 9 out of the 12 molecules with calculated χ-parameters (75%) were accurately predicted to either permeate or not, with 100% of molecules predicted to be permeable below our critical threshold ($\chi < 7.85$) proving to be permeable experimentally. In contrast, diffusion experiments showed that 10 out of the 16 total molecules (62.5%) were permeable in the nanoculture system.

Despite these limitations, the Flory-Huggins predictive model has proven to be accurate for a particular range of molecules, notably those with interaction parameters below the designated critical threshold. The accuracy of the predictive tool becomes less reliable as the interaction parameters increase, suggesting that improvements in methods for calculating HSPs for various molecules would certainly lead to improvements in subsequent predictive models, therefore, broadening the utility of the Flory-Huggins predictive model.

Developing such a predictive tool that could estimate the diffusion of a molecule based simply on chemical structure, would significantly increase our understanding of the transport phenomena surrounding PDMS membranes. Furthermore, it would substantially decrease experimental time if controls to test diffusion only could be negated based on the predictive power of the Flory-Huggins interaction parameter. A "catalogue" could be established, per se, of relevant molecules that could be used to control microbial dynamics either within or outside of the nanocultures with the use of a specified membrane type. Importantly, we might use predictive interaction parameters to explore secondary metabolic products that could diffuse out of the nanoculture and into the surrounding media, and the effects of such metabolites that shape community dynamics in the immediate environment. Such exploratory studies can be extended to drug discovery efforts when studying microbial populations from environmental samples. Moreover, understanding the diffusivity of fluorescent probes allows for contrast staining methods that could enhance visual assessment of cell dynamics, such as cell viability, metabolic activity, and enzymatic reactions. The development of nanocultures as 3D microbial assessment tools is part of our future work.

4-MATERIALS AND METHODS

4.1 Flory-Huggins calculations. A detailed description of the FH-interaction parameters and calculation thereof may be found in the Supporting Information. All Hansen Solubility Parameters and molar volumes of the solute molecules used in this article were kindly provided by Prof. Steven Abbott (HSPiP software), which were subsequently used in FH-interaction calculations. A theoretical critical interaction parameter of $\chi = 7.85$ (water-PDMS) was arbitrarily assigned to this system based on previous experiments, such that solutes with $\chi \leq 7.85$ were predicted to be diffusible, and those with $\chi > 7.85$ had uncertain diffusivity properties.

4.2 Fabrication of microfluidic devices. The fabrication of glass microfluidic devices is described by Utada *et al*.[37] and Niepa *et al*.[7] and was followed with slight modifications. Water-oil-water PDMS microcapsules were generated with the use of a microfluidic device with hydrodynamic flow-focusing and coflowing geometry. Briefly, two glass cylindrical tubes with inner and outer diameters of 0.58 mm and 1.03 mm (World Precision Instrument) were tapered and cut to the desired diameters using a Sutter P-1000 Horizontal Micropipette Puller (Sutter Instrument) and a MF-900 microforge (Narishige). The inner diameter of the tapered capillary for injection of the bacteria phase was 40 μm, and the outer surface of this same capillary was functionalized with 1% octadecyltrichlorosilane (OTS, Sigma-Aldrich) in toluene, to increase hydrophobicity of the glass surface. This chemical treatment enhances the wettability with PDMS and facilitates the formation of capsules. The inner diameter of the capillary for the collection of capsules is 200 μm. The two tapered capillaries were inserted into a glass, square capillary (inner dimension of 1.05 mm), and set 120 μm apart, with tapered openings facing towards each other. Transparent epoxy was used to attach, and seal blunt dispensing needles (20ga, 0.5”, Fisher Scientific) and polyethylene tubing (1.57 mm I.D., Scientific Commodities) to the glass capillaries for the injection and collection of liquid phases.

4.3 Microorganisms and growth conditions. Model organism *Escherichia coli* was used for the generation of all nanocultures for diffusion experiments. For all antibiotic diffusion experiments, except ampicillin, *E. coli* DH5-α pNCS-mClover 3 (amp^R) (Addgene[38]) was used; a strain that harbors a plasmid for the constitutive expression of GFP with resistance to antibiotic ampicillin. For the diffusion of ampicillin, specifically, *E. coli* Nissle pRSH103 RFP (tet^R) was used, which constitutively expresses RFP and harbors resistance to antibiotic tetracycline. For diffusion of

fluorescent probes, wild type *E. coli* Nissle 1917 (non-fluorescent) was used to generate nanocultures. For routine culturing, the cells were cultured for approximately 18 hours in an Erlenmeyer flask with 25 mL Ultra-filtered Tryptone-Yeast Extract (UFTYE) broth at 37°C, aerobically, with shaking. The UFTYE medium consisted of 2.5% tryptone, 1.5% yeast extract, and 1% glucose, and had a molecular-weight cutoff of 10 kDa (Millipore). 10 μL of the overnight culture was resuspended in 5 mL of sterile UFTYE medium to make the inner phase of the nanocultures. For diffusion of sugar molecules, DH5-α mApple-pBAD *E.coli* (Addgene[39]) was used to generate nanocultures. Overnight cultures were made as described above; however, prior to using in microfluidic experiments, the overnight culture was washed 3x with 154 mM NaCl to flush out any sources of carbon. The inner phase for these nanocultures was comprised of M9 minimal media (Sigma Aldrich), supplemented with trace vitamins (ATCC, Manassas, VA), $FeSO_4$ and $CaCl_2$ (Sigma Aldrich) ensuring that cells had all necessary growth factors to grow, bar carbon. 10 μL of the washed overnight culture was then resuspended in 5 mL of the supplemented minimal medium to make the inner phase of the nanocultures.

4.4 PDMS preparation. PDMS was prepared as previously described by Manimaran et al.[9] with modifications. Briefly, starting constituents were mixed with a magnetic stir-bar for 10 mins, comprised of vinyl-terminated polydimethylsiloxanes base (DMS-V21 Gelest Inc.) and cross-linker methylhydrosiloxane-dimethylsiloxane copolymer, trimethylsiloxy-terminated polydimethylsiloxanes (HMS-053, Gelest Inc.) to a ratio of 0.6 according to the concentration of their respective functional groups. Functional molecule N, N-Dimethylallylamine (DMAA, Fisher Scientific) was added to a final concentration of 10% of the functional group of competing vinyl DMS-V21. These molecules crosslink in the presence of platinum-divinyltetramethyldisiloxane, 2% Pt in xylene (Sigma-Aldrich), added to a final concentration of 1 ppm. This concentration allowed a working time of ~3 hours before crosslinking at room temperature (RT) occurred. The PDMS mixture was then degassed (Bel-Art™) for 10 minutes at RT prior to being used in microfluidic experiments.

4.5 Generation of nanocultures. The microfluidic device was mounted on an inverted optical microscope (Eclipse TE300, Nikon). The three fluid phases were delivered to the microfluidic device through polyethylene tubing (Scientific Commodities) attached to syringes (SGE) and driven by positive displacement syringe pumps (Harvard Apparatus, Standard PHD ULTRA™

CP). Droplet formation was monitored with a Phantom VEO 710 L high-speed camera (Vision Research) connected to the inverted microscope. The inner aqueous phase consists of bacteria suspended in the culture medium; the middle phase consists of the PDMS mixture with HMS-053 and DMS-V21 at a molar ratio of 0.6:1, supplemented with 1 ppm Pt (Gelest). The outer phase is 2 wt% poly(vinyl alcohol) aqueous solution (PVA, 87–89% hydrolyzed, average M_w = 31,000–50,000, Sigma Aldrich). The nanocultures were generated with a suspension of *E. coli* cells in the chosen media (UFTYE or M9 minimal) as the inner phase of the flow-focusing microfluidics device. The nanocultures were seeded at an average density of 0-5 cells per nanoculture and collected in UFTYE or M9 minimal medium. The capsules were heat-treated at 70°C for 5 min to catalyze crosslinking before their incubation at 37°C overnight.

4.6 Diffusion of antibiotics. Stock solutions of all antibiotics were prepared according to manufacturer's protocols. Ampicillin, hydrogen peroxide and tetracycline were acquired from Fisher Scientific BioReagents. Chloramphenicol and ofloxacin were acquired from Sigma Aldrich. Tobramycin was acquired from Acros Organics. Minimum inhibitory concentration growth curves were performed for all test antimicrobials against the corresponding bacterial strain to be used in the generation of nanocultures. Briefly, antimicrobials were serially diluted in 96-well plates with UFTYE medium. Overnight bacterial cultures were washed three times (6000g, 10 mins) in 154 mM NaCl, and were diluted to an OD_{600} of 0.5, prior to being pipetted into the 96-well plate. Absorbance of the bacterial cultures was monitored at a wavelength of 600 nm, for 48 hours. Nanocultures were generated and collected in small Petri dishes (3 mm diameter) containing UFTYE medium and subsequently heat treated for 5 mins at 70°C. A short period of heat treatment helps to initiate polymeric crosslinking of the nanoculture shell with no significant effects on microbial growth dynamics.[8] Test antimicrobials were added to each collection dish for final concentrations ranging from 0 – 16 mM. The nanocultures were then incubated overnight for 24 hours aerobically at 37°C. The following day, the nanocultures were imaged using a Zeiss Axio Imager M2 Epifluorescence and Brightfield Microscope (Carl Zeiss, Inc., Germany). Florescent images were taken at 10× magnification of the nanocultures to analyze mean florescence intensity of the cells in the nanocultures, at every drug concentration.

4.7 Diffusion of fluorescent dyes. Stock solutions of all fluorescent dyes were prepared according to manufacturer's protocols. Nanocultures were generated with *E. coli* Nissle 1917 (WT) and

collected in small Petri dishes (3 mm diameter) containing UFTYE medium and 50 μg/mL of antibiotic tobramycin, which maintains sterility of the collection media external to the nanocultures during incubation. The nanocultures were subsequently heat treated for 5 mins at 70℃ to initiate crosslinking of the polymeric membrane. Then, the nanocultures were incubated in a stationary incubator overnight for 24 hours to achieve cell confluence within the nanocultures. Subsequent staining of the cells was achieved by adding the selected fluorescent dyes to the collection media. Propidium iodide and Syto 9 (1.5 μL/mL each, Invitrogen Thermo Fisher Scientific) were used in conjunction in samples, since they are collectively used for live/dead assays. Acridine Orange (15 μM, Invitrogen Thermo Fisher Scientific), Crystal Violet (0.5% v/v, Electron Microscopy Sciences), Nile blue (25 μM, Sigma Aldrich) and Nile red (25 μM, Sigma Aldrich) were each used in separate samples. After adding the fluorescent probes to the nanoculture suspensions, the samples were covered with foil to prevent degradation of light-sensitive dyes and were left to incubate for 30 mins at RT. Samples were then imaged with a Zeiss Axio Imager M2 Epifluorescence and Brightfield Microscope (Carl Zeiss, Inc., Germany). Florescent images were taken at 50× magnification of the nanocultures to qualitatively assess diffusion of florescent dyes into the nanocultures. A time-lapse was performed for diffusion of AO, because the dye was not initially permeable after 30 minutes. The time-lapse was observed for 24 hours at 10 second intervals, monitoring change in green and red fluorescence within the nanoculture. Mean fluorescence intensity of the nanocultures was analyzed in ImageJ.

4.8 Diffusion of sugar molecules. Stock solutions of the sugar molecules were prepared by mixing glucose, sucrose, or arabinose with sterile distilled water. For glucose (Alfa Aesar) and sucrose (Fisher Scientific) diffusion experiments, nanocultures were generated with DH5-α mApple-pBAD *E. coli* in M9 media with supplemented trace vitamins (ATCC, Manassas, VA), $FeSO_4$ and $CaCl_2$, and collected in small Petri dishes (3 mm diameter) containing the same supplemented M9 media, and further supplemented with the test sugar molecule ranging in concentrations from 0-10% (v/v). 50 μg/mL of antibiotic tobramycin was also added to the collection media to maintain sterility in the external environment during incubation. The nanocultures were heat treated for 5 mins at 70℃, prior to being incubated at 37℃ aerobically and stationary, for 48 hours. A short period of heat treatment helps to initiate polymeric crosslinking of the nanoculture shell. For diffusion of arabinose (Acros Organics), nanocultures were generated with DH5-α mApple-pBAD *E. coli* in UFTYE media and collected in UFTYE media with 50 μg/mL of antibiotic tobramycin.

Nanocultures were heat treated for 5 mins at 70°C. Then, the test molecule, arabinose (100 µg/mL), was added to the external collection media and nanocultures were incubated at 37°C aerobically for 24 hours. Nanocultures were imaged at 10× for fluorescence intensity and mean florescence intensity was analyzed in ImageJ.

4.9 Diffusion of Lactic acid. Stock solutions of lactic acid (Sigma Aldrich) were prepared according to manufacturer's protocols. Nanocultures were generated with 0.1 M NaOH (Fisher Scientific) supplemented with 1 mg/mL Thymol Blue (Sigma Aldrich) and having varied shell thickness, and then collected in 0.1 M NaCl solution in small Petri dishes (3 mm diameter). Following generation, nanocultures were heat treated for 5 mins at 70°C to initiate crosslinking. Lactic acid was then added to the external collection solution to a final concentration of 0.2 M. A time-lapse was recorded at 10 second intervals to capture the color change from blue to yellow as diffusion occurred. Color change was analyzed in ImageJ by measuring RGB channel intensity.

4.10 Varying Hansen Solubility Parameters for PDMS. Hypothetical Flory-Huggins interaction parameters (χ) were calculated for the solute-polymer pairs based on changing the HSP value of the polymer. The HSP for PDMS was altered by adding or subtracting integers in increments of 1 to the literature-determined value for PDMS (δ_{PDMS} = 14.932 $MP^{1/2}$), covering a wide range of HSP values for PDMS. Calculations were then performed as described in detail in the Supporting Information.

4.11 ImageJ Image Analysis for Mean Fluorescence Intensity. All images were analyzed in ImageJ (FIJI). Imported images were split by color channel before analysis. The "rolling ball" background subtraction algorithm was implemented on fluorescent images prior to analysis to correct for uneven illumination. The rolling ball diameter was set to 150 px for all images taken at 10X magnification for consistent analysis, representing a rolling ball of greater diameter than the nanocultures, whereby fluorescence intensity was of interest. Mean fluorescence intensity was measured for the entire 2D area of nanoculture, with the ROI lining the inner membrane surface. In each test, a minimum of 15 nanocultures (n=15) was analyzed for mean fluorescence intensity. Furthermore, five ROIs in each image were captured for background fluorescence. Fluorescence intensity for each object ROI was calculated using the "Corrected Total Cell Fluorescence" (CTCF) equation.

4.12 Statistical Analysis. All statistical analysis was conducted in GraphPad Prism Software (V8). Significance of testing conditions was tested by t-test, one-way and two-way ANOVA. Differences of $p < 0.05$ were considered statistically significant. The following notations: "ns", *, **, ***, and **** describe the statistical difference with p values corresponding with $p > 0.05$, $p < 0.05$, $p < 0.01$, $p < 0.001$, and $p < 0.0001$, respectively.

SUPPORTING INFORMATION

Determination of Flory-Huggins interaction parameter; antibiotic- induced growth inhibition of *E. coli* cells; controls for fluorescent probes minimal media growth curves for *E. coli* cells; and diffusion of sugar molecules.

ACKNOWLEDGEMENTS

We would also like to thank Professor Steven Abbott (HSPiP) for fruitful discussions regarding solute-polymer diffusion, and for providing all partial solute parameters and molar volumes for the solutes used in this study.

COMPETING INTERESTS

The authors declare that there are no competing interests.

AUTHOR CONTRIBUTION

Corresponding Author

Tagbo H. R. Niepa - *Department of Chemical and Petroleum Engineering, Department of Bioengineering, Department of Civil and Environmental Engineering, Department of Mechanical Engineering and Materials Science, Center for Medicine and the Microbiome, and McGowan Institute for Regenerative Medicine, University of Pittsburgh, Pittsburgh, Pennsylvania 15261, United States;* orcid.org/0000-0002- 3018-5419; Email: tniepa@pitt.edu

Author

Shanna-Leigh Davidson − *Department of Chemical and Petroleum Engineering, University of Pittsburgh, Pittsburgh, Pennsylvania 15261, United States;* orcid.org/0000-0002-9820-7397

Author Contributions

S-L.D. and T.H.R.N. conceived, designed, wrote the article, and designed the figures. All authors have critically reviewed and given approval to the final version of the manuscript.

Funding

This work was supported by the StartUp Funds from the University of Pittsburgh. T.H.R.N received funding from the United States National Science Foundation through Grant No. DMR-2104731.

REFERENCES

1. Wessel, A. K.; Hmelo, L.; Parsek, M. R.; Whiteley, M., Going local: technologies for exploring bacterial microenvironments. *Nature Reviews Microbiology* **2013,** *11* (5), 337-348.
2. Weibel, D. B.; Diluzio, W. R.; Whitesides, G. M., Microfabrication meets microbiology. *Nat Rev Microbiol* **2007,** *5* (3), 209-18.
3. Ahmed, T.; Shimizu, T. S.; Stocker, R., Microfluidics for bacterial chemotaxis. *Integrative Biology* **2010,** *2* (11-12), 604-629.
4. Schachter, B., Slimy business—the biotechnology of biofilms. *Nature Biotechnology* **2003,** *21* (4), 361-365.
5. Zengler, K.; Toledo, G.; Rappé, M.; Elkins, J.; Mathur, E. J.; Short, J. M.; Keller, M., Cultivating the uncultured. *Proceedings of the National Academy of Sciences* **2002,** *99* (24), 15681-15686.
6. Whitesides, G. M., The origins and the future of microfluidics. *Nature* **2006,** *442* (7101), 368-373.
7. Niepa, T. H.; Hou, L.; Jiang, H.; Goulian, M.; Koo, H.; Stebe, K. J.; Lee, D., Microbial Nanoculture as an Artificial Microniche. *Sci Rep* **2016,** *6*, 30578.

8. Usman, H.; Davidson, S.-L.; Manimaran, N. H.; Nguyen, J. T.; Bah, A.; Seth, R.; Beckman, E.; Niepa, T. H. R., Design of a well-defined poly(dimethylsiloxane)-based microbial nanoculture system. *Materials Today Communications* **2021,** *27*, 102185.

9. Manimaran, N. H.; Usman, H.; Kamga, K. L.; Davidson, S.-L.; Beckman, E.; Niepa, T. H. R., Developing a Functional Poly(dimethylsiloxane)-Based Microbial Nanoculture System Using Dimethylallylamine. *ACS Applied Materials & Interfaces* **2020,** *12* (45), 50581-50591.

10. Flory, P. J., *Principles of Polymer Chemistry*. Cornell University Press: 1953; pp 497-502.

11. Young, R. J.; Lovell, P. A., *Introduction to polymers*. 3rd ed. ed.; CRC Press: Boca Raton, 2011; pp 239-253.

12. Wang, D.-M.; Wang, C.-Y.; Chu, C.-Y.; Yeh, H.-M., Permeation of drug and swelling agent through polymeric membranes. *AIChE Journal* **2000,** *46* (12), 2383-2394.

13. Buxton, G. A.; Clarke, N., Drug diffusion from polymer core–shell nanoparticles. *Soft Matter* **2007,** *3* (12), 1513-1517.

14. Thakral, S.; Thakral, N. K., Prediction of Drug–Polymer Miscibility through the use of Solubility Parameter based Flory–Huggins Interaction Parameter and the Experimental Validation: PEG as Model Polymer. *Journal of Pharmaceutical Sciences* **2013,** *102* (7), 2254-2263.

15. Meng, F.; Dave, V.; Chauhan, H., Qualitative and quantitative methods to determine miscibility in amorphous drug–polymer systems. *European Journal of Pharmaceutical Sciences* **2015,** *77*, 106-111.

16. Alhalaweh, A.; Alzghoul, A.; Kaialy, W., Data mining of solubility parameters for computational prediction of drug-excipient miscibility. *Drug Development & Industrial Pharmacy* **2014,** *40* (7), 904-909.

17. Hansen, C. M., *Hansen solubility parameters : a user's handbook*. 2nd ed. / Charles M. Hansen. ed.; CRC Press: Boca Raton, 2007; pp 95-109.

18. Stefanis, E.; Panayiotou, C., Prediction of Hansen Solubility Parameters with a New Group-Contribution Method. *International journal of thermophysics* **2008,** *29* (2), 568-585.

19. Stefanis, E.; Panayiotou, C., A new expanded solubility parameter approach. *International journal of pharmaceutics* **2012,** *426* (1-2), 29-43.

20. Marsac, P. J.; Li, T.; Taylor, L. S., Estimation of Drug–Polymer Miscibility and Solubility in Amorphous Solid Dispersions Using Experimentally Determined Interaction Parameters. *Pharmaceutical Research* **2008,** *26* (1), 139.

21. Lee, J. N.; Park, C.; Whitesides, G. M., Solvent Compatibility of Poly(dimethylsiloxane)-Based Microfluidic Devices. *Analytical Chemistry* **2003,** *75* (23), 6544-6554.

22. Fedors, R. F., A method for estimating both the solubility parameters and molar volumes of liquids. *Polymer engineering and science* **1974,** *14* (2), 147-154.

23. Barton, A. F. M., *CRC handbook of solubility parameters and other cohesion parameters*. 2nd ed. ed.; CRC Press: Boca Raton, 1991; pp 405-430.

24. Hildebrand, J. H., An Improvement in the Theory of Regular Solutions. *Proceedings of the National Academy of Sciences - PNAS* **1979,** *76* (12), 6040-6041.

25. Van Krevelen, D. W.; Te Nijenhuis, K., *Properties of polymers: their correlation with chemical structure; their numerical estimation and prediction from additive group contributions*. Elsevier: 2009; pp 654-674.

26. Durkee, J. B., *Cleaning with solvents : science and technology*. William Andrew: Oxford, 2014; pp 654-674.

27. Chakrabarti, A.; Choi, G. P. T.; Mahadevan, L., Self-Excited Motions of Volatile Drops on Swellable Sheets. *Physical review letters* **2020,** *124* (25), 258002-258002.

28. Borde, A.; Larsson, M.; Odelberg, Y.; Hagman, J.; Löwenhielm, P.; Larsson, A., Increased water transport in PDMS silicone films by addition of excipients. *Acta biomaterialia* **2012,** *8* (2), 579-588.

29. Ramijan, K.; Ultee, E.; Willemse, J.; Zhang, Z.; Wondergem, J. A. J.; van der Meij, A.; Heinrich, D.; Briegel, A.; van Wezel, G. P.; Claessen, D., Stress-induced formation of cell wall-deficient cells in filamentous actinomycetes. *Nature Communications* **2018,** *9* (1), 5164.

30. Emerson, J. B.; Adams, R. I.; Román, C. M. B.; Brooks, B.; Coil, D. A.; Dahlhausen, K.; Ganz, H. H.; Hartmann, E. M.; Hsu, T.; Justice, N. B.; Paulino-Lima, I. G.; Luongo, J. C.; Lymperopoulou, D. S.; Gomez-Silvan, C.; Rothschild-Mancinelli, B.; Balk, M.; Huttenhower, C.; Nocker, A.; Vaishampayan, P.; Rothschild, L. J., Schrödinger's microbes: Tools for distinguishing the living from the dead in microbial ecosystems. *Microbiome* **2017,** *5* (1), 86.

31. Sabnis, R. W., *Handbook of Fluorescent Dyes and Probes*. John Wiley & Sons, Incorporated: New York, UNITED STATES, 2015.

32. Pierzyńska-Mach, A.; Janowski, P. A.; Dobrucki, J. W., Evaluation of acridine orange, LysoTracker Red, and quinacrine as fluorescent probes for long-term tracking of acidic vesicles. *Cytometry. Part A* **2014,** *85* (8), 729-737.

33. Du Plessis, J.; Pugh, W. J.; Judefeind, A.; Hadgraft, J., The effect of the nature of H-bonding groups on diffusion through PDMS membranes saturated with octanol and toluene. *European Journal of Pharmaceutical Sciences* **2002,** *15* (1), 63-69.

34. Zhang, J.; Sun, M.; Fan, A.; Wang, Z.; Zhao, Y., The effect of solute–membrane interaction on solute permeation under supersaturated conditions. *International Journal of Pharmaceutics* **2013,** *441* (1), 389-394.

35. Reis, J. A.; Paula, A. T.; Casarotti, S. N.; Penna, A. L. B., Lactic Acid Bacteria Antimicrobial Compounds: Characteristics and Applications. *Food Engineering Reviews* **2012,** *4* (2), 124-140.

36. Mathur, H.; Beresford, T. P.; Cotter, P. D., Health Benefits of Lactic Acid Bacteria (LAB) Fermentates. *Nutrients* **2020,** *12* (6), 1679.

37. Utada, A. S.; Lorenceau, E.; Link, D. R.; Kaplan, P. D.; Stone, H. A.; Weitz, D. A., Monodisperse Double Emulsions Generated from a Microcapillary Device. *Science (American Association for the Advancement of Science)* **2005,** *308* (5721), 537-541.

38. Bajar, B. T.; Wang, E. S.; Lam, A. J.; Kim, B. B.; Jacobs, C. L.; Howe, E. S.; Davidson, M. W.; Lin, M. Z.; Chu, J., Improving brightness and photostability of green and red fluorescent proteins for live cell imaging and FRET reporting. *Sci Rep* **2016,** *6*, 20889.

39. Shaner, N. C.; Lin, M. Z.; McKeown, M. R.; Steinbach, P. A.; Hazelwood, K. L.; Davidson, M. W.; Tsien, R. Y., Improving the photostability of bright monomeric orange and red fluorescent proteins. *Nat Methods* **2008,** *5* (6), 545-51.

Graphic for manuscript

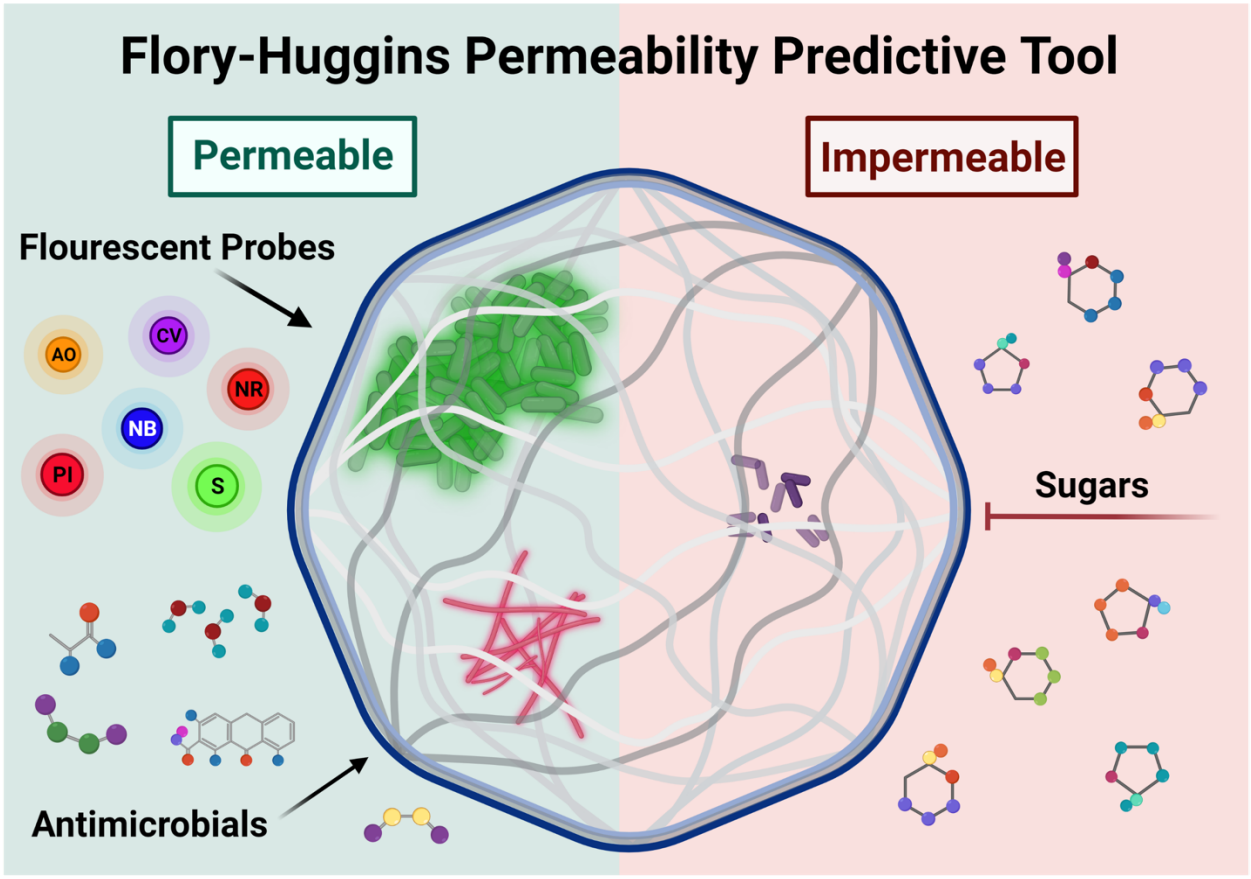

Supporting Information

Controlling Microbial Dynamics through Selective Solute Transport Across Functional Nanocultures

Shanna-Leigh Davidson[1], Tagbo H.R. Niepa[1,2,3,4,5,6]*

[1]Department of Chemical and Petroleum Engineering, [2]Department of Bioengineering; [3]Department of Civil and Environmental Engineering; [4]Department of Mechanical Engineering and Materials Science; [5]Center for Medicine and the Microbiome, [6]McGowan Institute for Regenerative Medicine, University of Pittsburgh, Pittsburgh, United States

*Corresponding author: tniepa@pitt.edu

Keywords: microbial dynamics, microfluidics, nanocultures, poly(dimethylsiloxane), chemical functionalization, Flory-Huggins.

This supplementary information provides evidence for supporting experiments complementary to the research article. Here, we have included a detailed discussion on finding Flory-Huggins interaction parameters for solute-polymer pairs. We further include bacterial growth curves to show inhibitory behavior of selected antimicrobial molecules. We show optimization of growth of bacteria in minimal media to determine successful growth in selected media. Figures complementary to sugar diffusion have also been included.

1. Determination of Flory-Huggins Interaction Parameter

Solubility between two molecules is often described by the cohesive energy density (CED) of each molecule, a value associated with the intermolecular attractive forces per unit volume of material. Subsequently, solubility occurs when two materials exhibit similar CEDs, such that the attractive intermolecular forces are overcome, and solvation may occur. The CED can be further described by the total solubility parameter, or Hildebrand value (Equation 1):

$$\delta = CED^{\frac{1}{2}} = \left(-\frac{U}{V}\right)^{\frac{1}{2}} \qquad (1)$$

where U is the molar internal energy (cal/mol) and V is the molar volume (cm^3/mol). The Hildebrand solubility parameter has been extensively used to predict polymer solubility (or swelling behavior) in non-polar solvents with great success.[1-3] Subsequently, attempts have recently been made to investigate the applicability of using Hildebrand solubility parameters to predict the solubility behavior of binary and multicomponent polymer-drug solution.[4-8] In these cases, the Flory-Huggins solution theory has been used with modifications to describe the Gibbs free energy of a drug-polymer binary system; the theory of which has been discussed extensively elsewhere.[1, 9, 10] The Flory-Huggins interaction parameter between drug and polymer thus arises out of the equation for Gibbs free energy, and provides an estimation of whether a solute will preferably partition into the polymer phase or not. The Flory-Huggins interaction parameter, χ, depends on the solubility parameters, δ, of both the solute (component 1) and polymer (component 2) as in the relationship (Equation 2):

$$\chi = \frac{V_1(\delta_1 - \delta_2)^2}{RT} \qquad (2)$$

where V_1 is the molar volume of component 1, R is the real gas constant in appropriate units, and T is the absolute temperature. A small interaction parameter typically indicates solubility; when δ_1 and δ_2 are similar, "like dissolves like" and it is predicted that the solute will partition and permeate through the polymer.

Although many advances have been made to understand relative interactions between drug-polymer blends, it is difficult to predict the solubility behavior of these systems because solubility parameters are not commonly known for molecules of biological interest, such as antimicrobials and the fluorescent dyes chosen for this study. Whereas solubility parameters for low molecular weight liquids can be conveniently found experimentally by obtaining the heat of vaporization, such direct methods do not work for high molecular weight polymers and crystal powders due to their low volatility. Hence, a common indirect method for estimating δ for such materials is based on Fedor's group contribution "molar-attraction constants" method, whereby only the chemical structure of the material is needed to sum the molar attractions of each functional group. Since the development of the group contributions method, it has evolved through many iterations to become an accurate tool in estimating several thermodynamic properties of compounds.[11-14]

One crucial enhancement to the applicability of Hilderbrand's total solubility parameter was the development of Hansen's partial solubility parameters, which better describe the different intermolecular forces governing a molecule. It is now widely understood that three kinds of intermolecular forces exist: dispersive, polar and hydrogen-bonding forces, all of which play an integral role in the thermodynamic properties of materials. Thus, the total solubility parameter, δ_t, is expanded upon as in Equation 3:

$$\delta_t = \sqrt{\delta_d^2 + \delta_p^2 + \delta_h^2} \qquad (3)$$

where δ_d represents dispersive forces, δ_p represents polar forces and δ_h describes hydrogen bonding forces. Accounting for these three forces results in a significantly more accurate estimate for the total solubility parameter and subsequently the predictive power of the Flory-Huggins interaction parameter has larger capacity.

Solubility parameters are subsequently used in the calculation of Flory-Huggins interaction parameters to predict miscibility of the solute in the polymer. For miscibility to remain thermodynamically favorable, χ must be small; however, the theoretical critical threshold for solubility is system specific, dependent on how the polymer volume lattice is defined.[15] All values calculated for the solute-nanoculture system have been reported in **Table 1** in the research article.

2. Antibiotic-induced growth inhibition of *E. coli* cells

Escherichia coli cells used for this study were tested for susceptibility to selected antimicrobials. For all antibiotic molecules, bar ampicillin, *E. coli* DH5-α pNCS-mClover 3 (amp^R) (*E. coli* GFP) was the selected bacterial strain. For ampicillin specifically, *E. coli* Nissle pRSH103 RFP (tet^R) (*E. coli* RFP) was the selected bacterial strain. In all cases, bacteria were grown in 200 μL UFTYE media in the presence of antibiotic molecules in a 96-well plate assay for 48 hours at 37 °C in aerobic conditions. Absorbance was measured every 10 minutes at OD_{600} using a 96-well plate reader (Cytation 5 imaging reader, BioTek Instruments Inc.) Antibiotic molecules ampicillin, chloramphenicol, ofloxacin and tetracycline were tested at concentrations ranging from 0 to 75 μM, and hydrogen peroxide was tested from 0-64 mM (**Figure S1**). In all cases, *E. coli* proved susceptible to the antibiotics at higher tested concentrations, and therefore, high cell fluorescence measurements within nanocultures are indicative of impermeability of the drug through the polymer shell.

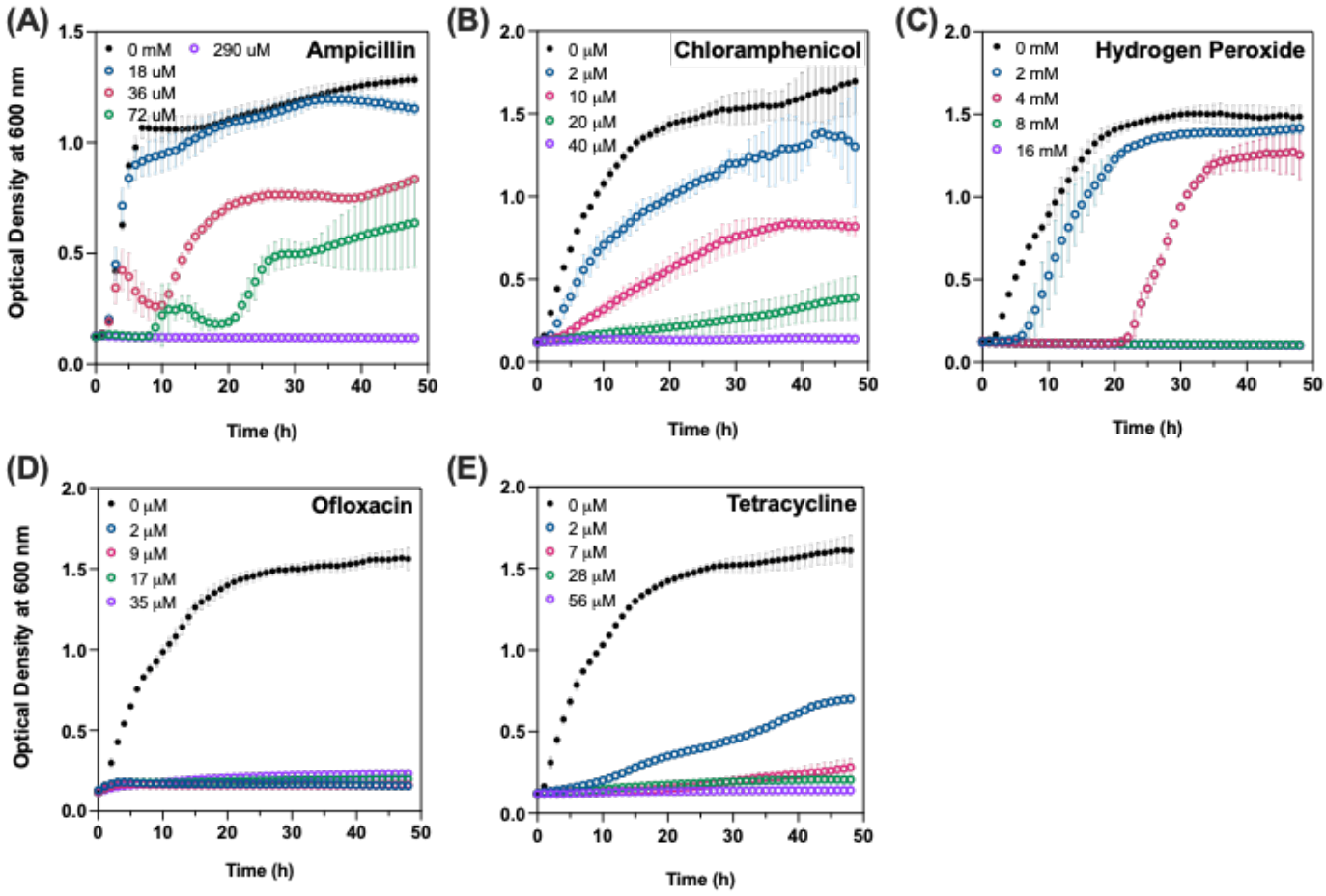

Figure S1. Growth inhibition curves with antimicrobials. **(A)** *E. coli* Nissle pRSH103 RFP (tet^R) (*E. coli* RFP) tested for susceptibility to ampicillin for diffusion test. *E. coli* mClover 3 (amp^R) (*E. coli* GFP) was tested against **(B)** chloramphenicol; **(C)** hydrogen peroxide; **(D)** ofloxacin; and **(E)** tetracycline in concentrations ranging from 0-200 µg/mL, to determine the minimum inhibitory concentration of each of antimicrobial. Hydrogen peroxide was tested in concentrations ranging from 0–64 mM. Growth inhibition of cells was achieved in each case, and appropriate antimicrobial concentrations were then selected for diffusion tests.

3. Controls for fluorescent probes

To ensure that the fluorescent dyes were all working as intended to dye the bacterial cells within the nanocultures, cells that were not encapsulated were stained as per manufacturer's protocols. *Escherichia coli* Nissle WT (non-fluorescent wild type) cells were allowed to adhere to glass cover slips and were then stained with the fluorescent stains: crystal violet (0.5% v/v), Nile blue (25 µM), Nile red (25 µM) (**Figure S2**), and Acridine Orange (15 µM) (**Figure S3**). Cells were incubated with the fluorescent dyes for 30 mins at room temperature and were then imaged at 50× under brightfield and fluorescent channels.

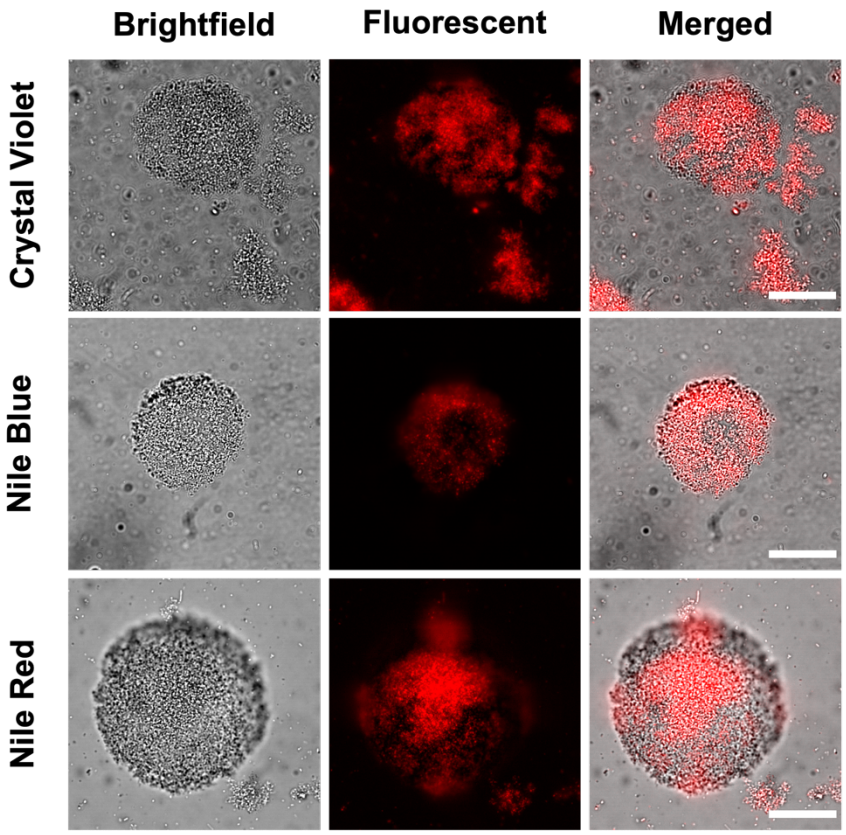

Figure S2. Controls for fluorescent probe staining of *E. coli* cells. Fluorescent and brightfield images taken at 50× show that crystal violet (0.5%), Nile blue and Nile red (25 μM) readily stain non-encapsulated cells. Scale bar: 50 μm.

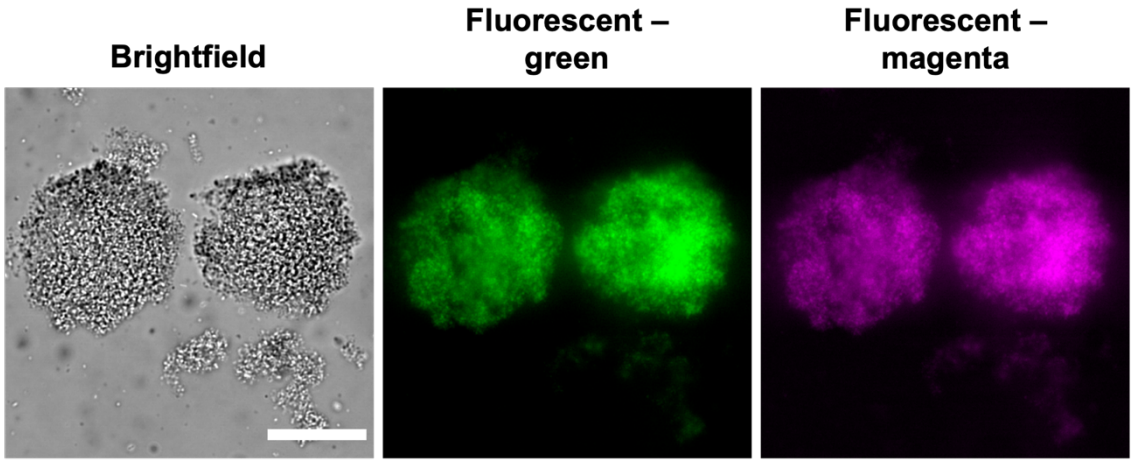

Figure S3. Controls for fluorescent probe (Acridine Orange) staining of *E. coli* cells. Brightfield and Fluorescent images taken at 50× show that Acridine Orange (15 μM) readily stains non-encapsulated cells. Green and Magenta images depict staining of double and single stranded nucleic acids, respectively. Scale bar = 50 μm.

4. Minimal media *E. coli* growth curves

Prior to testing the diffusion of sugar molecules within the nanocultures, we performed growth curves for four strains of *E. coli* each in four variations of minimal media, supplemented with 1% Trace Vitamins (ATCC) and 1% glucose, the purpose of which was to demonstrate that optimal conditions were achieved for confluent cell growth. The four strains of *E. coli* selected for optimizing cell growth included *E. coli* Nissle wild type (WT), DH5-α, mClover (*E. coli* GFP), and mApple (*E. coli* RFP). The growth assay contained cells grown in 200 µL of minimal media for 48 hours at 37 °C in aerobic conditions. Absorbance was measured every 10 minutes at OD_{600} using a 96-well plate reader (Cytation 5 imaging reader, BioTek Instruments Inc.). The growth curves demonstrated that most strains required longer than 24 hours for

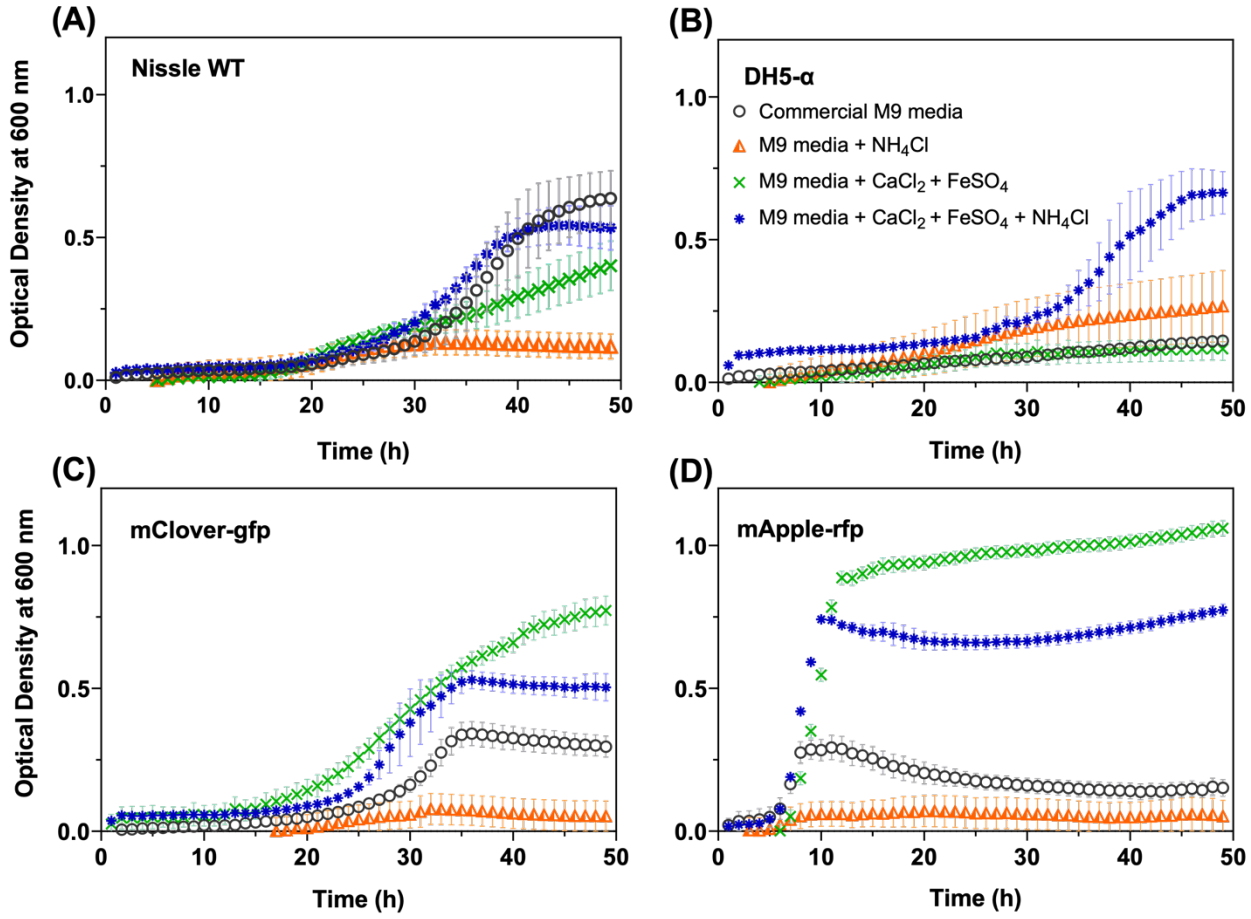

Figure S4. Growth curve optimization of *E. coli* strains in varying combinations of minimal media. Commercial M9 minimal media was supplemented in stages with 10 mM NH_4Cl, 0.1% $CaCl_2$, and 0.1% $FeSO_4$. All four versions of minimal media also included 1% trace vitamins and 1% glucose. Four *E. coli* strains were tested in the four variations of media, including **(A)** Nissle WT, **(B)** DH5-α, **(C)** mClover GFP, and **(D)** mApple RFP. *E. coli* mApple RFP performed the best in minimal media supplemented with $CaCl_2$ and $FeSO_4$, reaching approximately 0.8 OD_{600} after 12 hours of growth.

sufficient growth to be seen, and furthermore, that addition of only NH_4Cl to minimal media hindered cell growth in most cases (**Figure S4**). However, *E. coli* mApple (RFP) demonstrated successful growth within 13 hours when grown in minimal media supplemented with $CaCl_2$, $FeSO_4$, 1% trace vitamins, and 1% glucose. Subsequently, the combination of *E. coli* mApple (RFP) and minimal media supplemented with $CaCl_2$, $FeSO_4$, and 1% trace vitamins was selected for the core in nanoculture encapsulation. The test sugar molecules were then added to the external collection solution to determine diffusion.

5. Diffusion of sugar molecules

a. Glucose and Sucrose

After selecting the appropriate strain and minimal media that would ensure cell growth in the presence of a carbon source in the nanocultures, diffusion of glucose and sucrose across the nanoculture membrane was tested as described. In all cases, we observed no cell growth within the nanocultures, observed after 24 hours and again at 48 hours. This indicates that both sugar molecules are impermeable through the nanoculture membrane. **Figure S5** show representative images taken at 50× using a Zeiss Axio Imager M2 Epifluorescence and Brightfield Microscope (Carl Zeiss, Inc., Germany).

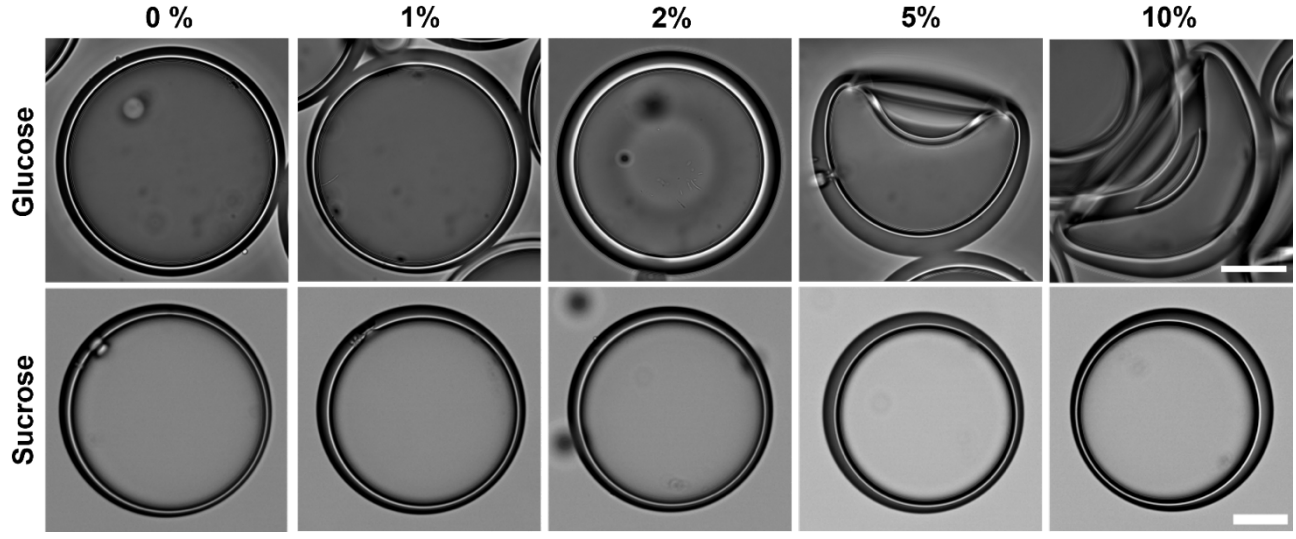

Figure S5. Diffusion of glucose and sucrose molecules through nanocultures membranes. Brightfield imaging showed no cell growth at all, imaged after 24 hours and again at 48 hours. Glucose and sucrose are unable to diffuse through the nanoculture membrane. Images taken at 50×, scale bar = 50 μm.

b. Arabinose

To demonstrate the diffusion of arabinose, mean fluorescence intensity was measured within the nanocultures. Positive (100 µg/mL arabinose) and negative (0 µg/mL arabinose) controls were included for the comparison of mean fluorescence intensity. In the test sample, 100 µg/mL arabinose was added to the external collection solution. After 24 hours incubation at 37 °C, mean fluorescence intensity was measured and analyzed in software package ImageJ-FIJI. In the positive control, whereby 100 µg/mL arabinose was added to the encapsulated core media, we observed a significantly higher mean fluorescence intensity than both the negative control (no arabinose added to system) and the test sample ($p < 0.0001$), indicating that arabinose is impermeable through the nanoculture membrane. **Figure S5** show representative images taken at 50× using a Zeiss Axio Imager M2 Epifluorescence and Brightfield Microscope (Carl Zeiss, Inc., Germany).

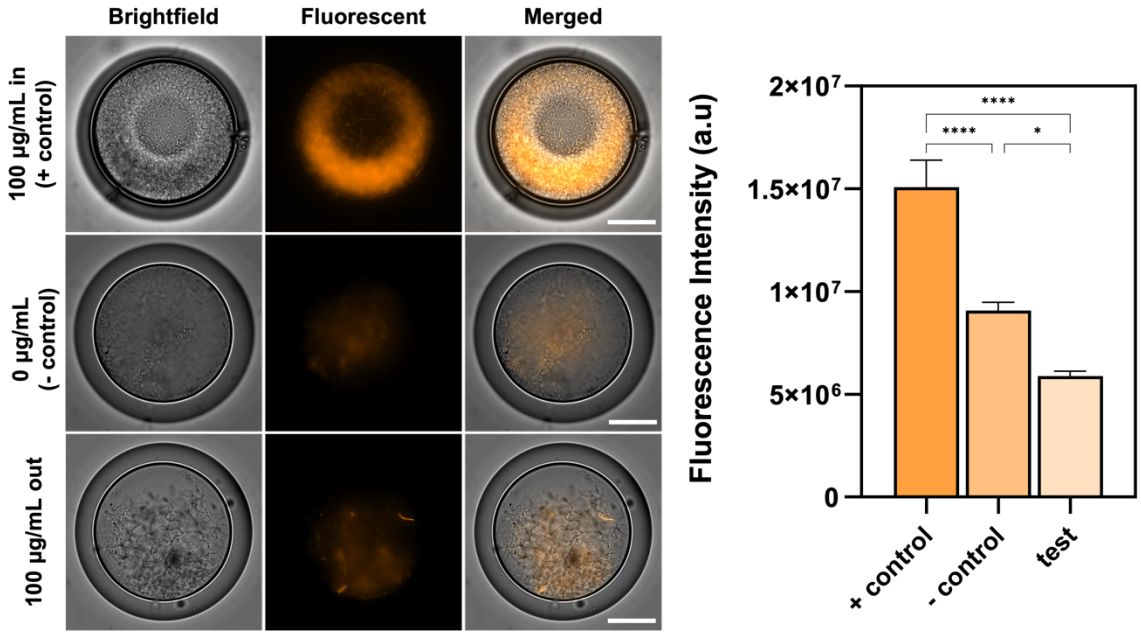

Figure S6. Diffusion of arabinose through nanoculture membrane. Diffusion of arabinose was investigated by proxy of fluorescence intensity of the mApple fluorescent protein which is induced by arabinose. Negative control had no arabinose added (0 µg/mL); baseline fluorescence is due to a leaky promoter. Positive control had 100 µg/mL arabinose added inside the capsule to compare fluorescence. The test sample had 100 µg/mL added externally to the capsule. Positive control had a statistically significant increase in mean fluorescence intensity, indicating that arabinose is impermeable through the nanoculture membrane. One-way ANOVA, Tukey post-hoc. Differences were considered significant when $p < 0.05$. **** significant at $p < 0.0001$. * Significant at $p = 0.0494$. Scale bar = 50 µm.

References

1. Hansen, C. M., *Hansen solubility parameters : a user's handbook*. 2nd ed. / Charles M. Hansen. ed.; CRC Press: Boca Raton, 2007.
2. Hildebrand, J. H., An Improvement in the Theory of Regular Solutions. *Proceedings of the National Academy of Sciences - PNAS* **1979,** *76* (12), 6040-6041.
3. Lee, J. N.; Park, C.; Whitesides, G. M., Solvent Compatibility of Poly(dimethylsiloxane)-Based Microfluidic Devices. *Analytical Chemistry* **2003,** *75* (23), 6544-6554.
4. Buxton, G. A.; Clarke, N., Drug diffusion from polymer core–shell nanoparticles. *Soft Matter* **2007,** *3* (12), 1513-1517.
5. Knopp, M. M.; Gannon, N.; Porsch, I.; Rask, M. B.; Olesen, N. E.; Langguth, P.; Holm, R.; Rades, T., A Promising New Method to Estimate Drug-Polymer Solubility at Room Temperature. *Journal of pharmaceutical sciences* **2016,** *105* (9), 2621-2624.
6. Mohammad, M. A.; Alhalaweh, A.; Velaga, S. P., Hansen solubility parameter as a tool to predict cocrystal formation. *International journal of pharmaceutics* **2011,** *407* (1), 63-71.
7. Niepa, T. H.; Hou, L.; Jiang, H.; Goulian, M.; Koo, H.; Stebe, K. J.; Lee, D., Microbial Nanoculture as an Artificial Microniche. *Sci Rep* **2016,** *6*, 30578.
8. Potter, C. B.; Davis, M. T.; Albadarin, A. B.; Walker, G. M., Investigation of the Dependence of the Flory–Huggins Interaction Parameter on Temperature and Composition in a Drug–Polymer System. *Molecular Pharmaceutics* **2018,** *15* (11), 5327-5335.
9. Flory, P. J., *Principles of Polymer Chemistry*. Cornell University Press: 1953.
10. Young, R. J.; Lovell, P. A., *Introduction to polymers*. 3rd ed. ed.; CRC Press: Boca Raton, 2011.
11. Fedors, R. F., A method for estimating both the solubility parameters and molar volumes of liquids. *Polymer engineering and science* **1974,** *14* (2), 147-154.
12. Hoy, K. L., *The Hoy tables of solubility parameters*. Union Carbide Corporation, Solvents & Coatings Materials, Research : 1985.
13. Stefanis, E.; Panayiotou, C., Prediction of Hansen Solubility Parameters with a New Group-Contribution Method. *International journal of thermophysics* **2008,** *29* (2), 568-585.
14. Van Krevelen, D. W.; Te Nijenhuis, K., *Properties of polymers: their correlation with chemical structure; their numerical estimation and prediction from additive group contributions*. Elsevier: 2009.
15. Marsac, P. J.; Li, T.; Taylor, L. S., Estimation of Drug–Polymer Miscibility and Solubility in Amorphous Solid Dispersions Using Experimentally Determined Interaction Parameters. *Pharmaceutical Research* **2008,** *26* (1), 139.